Journal of King Saud University Computer and Information Sciences (2026) 38:681
https://doi.org/10.1007/s44443-026-01131-5

RESEARCH

Reverse mixed data sampling based on expectile regression for inflation at risk and economic growth modeling

Muhammad Sjahid Akbar[1] · Wisnowan Hendy Saputra[2] · Dedy Dwi Prastyo[1] · Anton Abdulbasah Kamil[3]

Received: 18 May 2026 / Accepted: 21 July 2026
© The Author(s) 2026

Abstract

This study proposes a Reverse Mixed Data Sampling based on Expectile Regression (R-MIDAS-ER) framework for modeling Inflation at Risk and examining the role of economic growth in inflation risk dynamics. The proposed model addresses two central challenges in macroeconomic risk modeling: the mixed-frequency structure between monthly inflation and quarterly macroeconomic indicators, and the need to capture heterogeneous effects across the conditional inflation distribution. By integrating the Reverse MIDAS structure with asymmetric least squares expectile estimation, the model enables low-frequency real-sector information, particularly quarterly GDP growth, to explain high-frequency monthly inflation without imposing artificial aggregation or interpolation. Numerical experiments are conducted under Gaussian, heavy-tailed, skewed, contaminated, and heteroskedastic residual scenarios to evaluate finite-sample performance and robustness. The results show that R-MIDAS-ER provides stable recovery of the mixed-frequency transmission mechanism and achieves competitive or superior expectile forecasting performance, especially in upper-tail inflation risk regions. The empirical application to Indonesian data from January 2001 to June 2024 further demonstrates that inflation, GDP growth, financial stress, and financial conditions exhibit asymmetric and heavy-tailed behavior, supporting the use of distributional modeling. The R-MIDAS-ER model identifies several historically meaningful high-risk inflation episodes and reveals that GDP growth has a stronger association with upper-tail inflation risk than with lower-tail conditions. Financial conditions also exhibit asymmetric effects across expectile levels. Overall, the proposed framework offers an interpretable and distribution-sensitive approach for monitoring inflation vulnerability in mixed-frequency macroeconomic environments.

Keywords Reverse MIDAS · Expectile Regression · Inflation at Risk · Economic growth · Financial stress index · Financial condition index

1 Introduction

A thorough understanding of future inflation risks has become a top priority for monetary authorities and economic policymakers globally, particularly in efforts to maintain price stability and public purchasing power. The concept of Inflation at Risk (IaR) has emerged as a crucial framework for measuring the potential for extreme inflationary pressures, going beyond mere conditional average predictions (Frascaroli & Nobrega 2019; Girdzijauskas et al. 2022; Krasniqi and Gara 2025). Initially, the development of IaR models relied heavily on information from financial indicators, such as the Financial Stress Index (FSI) or the Financial Condition Index (FCI), as the primary predictors (Mundra & Bicchal 2021; Monin 2019). The use of these financial indicators is based on the assumption that volatility in financial markets often precedes inflation movements,

✉ Muhammad Sjahid Akbar
m_sjahid_a@its.ac.id

Wisnowan Hendy Saputra
wisnowan.saputra@binus.ac.id

Dedy Dwi Prastyo
dd.prastyo@its.ac.id

Anton Abdulbasah Kamil
akamil@gelisim.edu.tr

[1] Department of Statistics, Institut Teknologi Sepuluh Nopember, Surabaya, Indonesia

[2] Department of Computer Science, Bina Nusantara University, Jakarta, Indonesia

[3] Faculty of Economics, Administrative and Social Sciences, Istanbul Gelisim University, Istanbul, Turkey

Published online: 19 August 2026

and is supported by the availability of financial data with the same observation frequency as inflation data, namely monthly (Monteforte & Moretti 2013; Famubode & Ali 2024; Li et al. 2025). This facilitates researchers in applying standard econometric models due to the absence of data synchronization constraints.

However, increasingly complex economic dynamics demonstrate that relying solely on financial indicators is insufficient to capture the full picture of risk (Arnold et al. 2012; Zakhidov 2024). Field realities demonstrate that real economic conditions, such as output and productivity growth, have a fundamental influence on inflation movements through various transmission mechanisms, including demand-pull and cost-push inflation mechanisms. Although the inclusion of macroeconomic variables is considered crucial for improving the accuracy of IaR estimates, integrating these variables faces significant methodological challenges (Carriero et al. 2019; Khan et al. 2024). The main problem lies in the stark contrast in data frequency. Inflation data is typically available monthly, while key economic indicators such as Gross Domestic Product (GDP) are only released quarterly (Saputra et al. 2024a). This frequency discrepancy makes classical linear regression-based modeling unsuitable directly, as traditional regression requires all variables to have the same number of observations and time units (Saputra et al. 2024b, 2025).

In addition to the constraints related to data frequency, another limitation arises from the use of average- or mean-based estimation methods such as Ordinary Least Squares (OLS). In the context of risk management, estimates at the midpoint of a distribution fail to provide insight into data behavior under extreme conditions (Sarkar et al. 2025; AboAlkhair et al. 2025). The essence of Inflation at Risk is the model's ability to capture information at the tail of the distribution (tail risk) to identify the probability of extremely high or extremely low inflation that could threaten economic stability (Almetwally et al. 2025). Therefore, an approach is needed that not only handles differences in data frequency elegantly but also estimates the relationships between variables at various risk levels without relying on the assumption of a normal distribution, which is often not met in real economic data characterized by heavy tails.

To address this challenge, this study proposes a novel approach by combining the Reverse Mixed Data Sampling (R-MIDAS) framework with estimation based on Expectile Regression (Xu et al. 2021; Sobotka & Kneib 2012). Using R-MIDAS allows researchers to incorporate information from low-frequency variables, such as quarterly economic growth, into the model to explain high-frequency variables, namely monthly inflation, without losing important information due to forced data aggregation. Meanwhile, Expectile Regression was chosen as the estimation tool based on its advantage in capturing distribution tail risks more sensitively than quantile regression, as it utilizes all information in the data distribution through an asymmetric least squares approach. The main novelty of this research lies in the development of a formal estimation procedure for the Reverse Mixed Data Sampling-Expectile Regression (R-MIDAS-ER) model, which until now has received very limited discussion in the applied econometrics literature.

The methodological and empirical innovations of this study extend far beyond a simple modification of the dependent variable in a standard regression framework. Methodologically, this study is the first to formally develop and evaluate the Reverse Mixed Data Sampling based on Expectile Regression (R-MIDAS-ER) model. While previous R-MIDAS literature has focused on conditional means or quantiles, we derive the exact analytical first-order gradients and second-order Hessian matrices for this integrated framework, proving its mathematical viability. More importantly, we identify and leverage a unique computational synergy between expectiles and non-linear MIDAS lag polynomials: the smooth, continuously differentiable L_2 loss of expectiles compensates for the non-convexity and non-linearity of the Almon lag structure, directly resolving the numerical convergence failures and local-minima traps that commonly plague non-smooth quantile-based MIDAS models (QADL-MIDAS). Furthermore, we integrate the Chernozhukov et al. (2010) post-estimation rearrangement operator directly into the R-MIDAS-ER pipeline, providing a novel, mathematically guaranteed solution to the expectile-crossing problem, ensuring logically consistent, monotone empirical risk surfaces.

Empirically, this model resolves a long-standing constraint in the Inflation at Risk (IaR) literature, which historically relied solely on financial indicators due to data frequency mismatches. By enabling the direct integration of quarterly GDP growth into monthly inflation risk modeling, our framework reveals a highly asymmetric, demand-pull transmission mechanism where real economic growth primarily drives upper-tail inflation risks while exerting negligible effects on lower-tail or average inflation—a critical structural insight that conventional mean-based or symmetric models fail to capture.

The robustness of the R-MIDAS-ER model proposed in this study was evaluated through two comprehensive testing stages. First, numerical experiments involving various residual distribution variations were conducted to test the model's ability to withstand and maintain accuracy under non-ideal data conditions or those deviating from the assumption of normality. Model performance was then measured using several evaluation metrics considered robust to data anomalies. Second, to demonstrate its practical relevance, the model was implemented in real-world Inflation at Risk modeling in Indonesia, using national economic growth as the primary predictor variable. Through its application to real Indonesian

data, this study is expected to provide empirical contributions to Bank Indonesia and the government in mapping future inflation risks more precisely, allowing for better formulation of anticipatory policies based on the dynamics of ongoing economic growth.

2 Related work

The concept of Inflation at Risk (IaR) has emerged as an increasingly important research agenda within modern macroeconomics and monetary economics, particularly following the growing recognition that inflation dynamics cannot be adequately understood solely through average-based forecasting approaches. Traditional inflation forecasting models have historically focused on estimating the conditional mean of inflation using linear econometric frameworks such as autoregressive models, Phillips curve specifications, vector autoregression (VAR), and dynamic stochastic general equilibrium (DSGE) models. While these approaches have proven useful for describing general inflation trends under normal economic conditions, they often fail to provide meaningful information regarding the probability and magnitude of extreme inflationary outcomes. Such limitations became particularly evident during episodes of severe economic disruption, including the Global Financial Crisis, the COVID-19 pandemic, energy price shocks, and post-pandemic supply-chain disruptions, where inflation distributions exhibited substantial asymmetry, volatility clustering, and heavy-tailed behavior. Consequently, policymakers and researchers increasingly shifted their attention toward distributional approaches capable of quantifying risks embedded within the tails of the inflation distribution rather than merely estimating expected inflation values.

The conceptual foundation of Inflation at Risk is closely related to the broader literature on macroeconomic tail-risk analysis, particularly the Growth at Risk (GaR) framework introduced by Adrian et al. (2019). Their influential work on vulnerable growth demonstrated that financial conditions contain substantial predictive power for downside macroeconomic risks and that examining only conditional means masks important information about economic vulnerabilities. This distributional perspective subsequently inspired the extension of tail-risk analysis toward inflation dynamics, leading to the development of Inflation at Risk as a framework for quantifying the probability of extreme inflation realizations under varying macroeconomic and financial conditions.

One of the pioneering and most influential contributions to the IaR literature was developed by Lopez-Salido and Loria (2024), who formally introduced the concept of Inflation at Risk using quantile regression methods applied to panels of OECD economies. Their study demonstrated that the tails of the inflation distribution exhibit substantial variability even during periods characterized by relatively stable average inflation. More importantly, they found that financial conditions exert nonlinear and asymmetric effects on inflation risk, implying that tightening financial conditions may amplify downside inflation risks during certain periods while contributing to upside risks in others. Their findings also revealed that the determinants of inflation risk evolve over time, suggesting that the structure of inflation dynamics is not stable across economic regimes. This contribution significantly advanced the literature by emphasizing that monetary authorities must monitor not only expected inflation but also the entire predictive distribution of inflation outcomes.

Subsequent studies expanded the Inflation at Risk framework by incorporating broader sets of explanatory variables and more sophisticated econometric methodologies. Research conducted by Banerjee et al. (2024) extended IaR analysis to both advanced and emerging market economies. Their work highlighted substantial heterogeneity in inflation risk transmission across countries, particularly between developed and emerging economies. In emerging market economies, exchange rate fluctuations and financial tightening were shown to generate stronger and more asymmetric inflation risks than in advanced economies. Additionally, the study documented that inflation-targeting regimes tend to reduce right-skewed inflation risk distributions, thereby improving inflation stability. These findings reinforced the argument that institutional structures, monetary policy credibility, and exchange rate exposure play fundamental roles in shaping inflation tail risks across different economic environments.

In emerging market economies, the exchange rate represents a primary channel of macroeconomic vulnerability. Fluctuations in the exchange rate feed directly into domestic price indices through import channels (exchange rate pass-through) and drastically amplify upper-tail inflation risks during periods of capital flight. Crucially, the literature on financial economics establishes that price indices and monetary factors do not evolve in isolation but are bound by deep, long-run structural co-movements with asset markets. For instance, Tsagkanos and Siriopoulos (2013) introduced a structural nonparametric cointegrating regression approach to demonstrate that the stock price index and the exchange rate exhibit significant, non-linear long-run relationships under regime shifts and macroeconomic distortions. This structural co-movement framework is highly relevant to emerging markets, where capital inflows, global host market shocks, and domestic asset prices interact dynamically. Under structural shifts, these financial co-movements directly propagate volatility into domestic price levels (CPI/inflation). Therefore, analyzing inflation tail risks in an emerging economy requires a framework that acknowledges

these underlying, long-run structural dependencies among exchange rates, asset prices, and inflation dynamics.

The evolution of the IaR literature has also been accompanied by growing methodological sophistication, particularly in the application of quantile-based econometric techniques. Quantile regression has become one of the dominant estimation tools within the IaR framework because it enables researchers to examine heterogeneous relationships between explanatory variables and different regions of the conditional inflation distribution. Unlike Ordinary Least Squares (OLS), which estimates only the conditional mean, quantile regression allows the effects of predictors to vary across lower, median, and upper quantiles. This capability is particularly important in inflation risk analysis because the determinants of extreme inflation outcomes may differ substantially from those influencing average inflation dynamics. Early contributions by Manzan and Zerom (2013) demonstrated that incorporating macroeconomic variables into quantile regression frameworks substantially improves inflation density forecasting performance relative to conventional approaches. Their findings showed that inflation dynamics are highly nonlinear and that the predictive relevance of macroeconomic variables changes across different regions of the inflation distribution.

In parallel, another important stream of the literature focused on integrating mixed-frequency data structures into inflation risk analysis. The motivation behind this development stems from the practical reality that macroeconomic indicators are often observed at different frequencies. Inflation is typically available monthly, whereas variables such as Gross Domestic Product (GDP), productivity, or national accounts data are generally published quarterly. This mismatch creates significant methodological challenges because conventional regression frameworks require synchronized observation frequencies. To address this issue, researchers increasingly adopted Mixed Data Sampling (MIDAS) methodologies, which allow variables observed at different frequencies to be incorporated into a unified econometric framework without requiring forced aggregation or interpolation.

One of the seminal contributions in this direction was developed by Ghysels et al. (2018), who introduced Quantile Autoregressive Distributed Lag MIDAS (QADL-MIDAS) models for inflation risk analysis. Their work demonstrated that mixed-frequency quantile regression models significantly outperform standard quantile autoregression approaches in forecasting inflation distributions across various horizons. More importantly, they showed that MIDAS-based risk measures provide meaningful information regarding inflation uncertainty, asymmetry, and the probability of extreme inflation realizations. This contribution represented an important methodological bridge between mixed-frequency econometrics and distributional risk analysis.

The broader mixed-frequency econometrics literature has also contributed substantially to improving inflation forecasting methodologies. Studies such as those by Omer et al. (2024) proposed improved estimators for mixed-frequency models using nonparametric shrinkage techniques instead of conventional Almon lag polynomials. Their findings suggested that flexible mixed-frequency estimators can enhance forecasting performance in inflation applications by capturing more complex lag structures embedded within macroeconomic relationships. Such developments are highly relevant for Inflation at Risk analysis because tail-risk dynamics are often sensitive to the timing and persistence of macroeconomic shocks.

Another important dimension within the IaR literature concerns the role of financial conditions and monetary policy transmission mechanisms. A substantial body of evidence suggests that financial markets contain valuable forward-looking information regarding future inflation risks. Tightening financial conditions may suppress aggregate demand and generate downside inflation risks, whereas accommodative financial conditions may stimulate excessive demand and amplify upside inflation pressures. Studies on macroeconomic risk forecasting demonstrated that financial conditions exert asymmetric effects on the distribution of macroeconomic variables, including inflation. In particular, tighter financial conditions are frequently associated with higher inflation uncertainty and increased tail risks. These findings support the broader argument that financial-sector vulnerabilities and inflation dynamics are deeply interconnected through nonlinear transmission channels (Adams et al. 2021).

Recent developments in the literature have further extended Inflation at Risk analysis into multidimensional and dynamic frameworks. For instance, newer studies introduced the concept of Growth and Inflation at Risk (GIaR), which jointly models downside growth risks and upside inflation risks within a unified framework. This approach is particularly relevant for analyzing stagflation scenarios, where economies simultaneously experience weak growth and elevated inflation. Such multidimensional tail-risk frameworks provide policymakers with more comprehensive assessments of macroeconomic vulnerabilities under adverse economic conditions (Corradi & Llorens-Terrazas 2026).

Despite these substantial advancements, several important research gaps remain unresolved within the existing literature. First, most existing Inflation at Risk (IaR) studies still rely heavily on quantile-based approaches (Lopez-Salido & Loria 2024). While quantile regression is valuable for estimating specific conditional thresholds, it possesses a notable limitation in risk management: it is purely position-based. It determines the probability of inflation exceeding a certain threshold (analogous to Value at Risk) but remains insensitive to the actual magnitude of extreme inflation

values beyond that threshold. In monetary policy, understanding not just whether inflation will breach a target but how severe the breach could be (the tail shape and scale) is critical for preparing stabilization policies. Expectile regression addresses this gap by utilizing an asymmetric quadratic loss function, making it sensitive to both the probability and the magnitude of tail realizations.

Therefore, the present study contributes to the literature by integrating Reverse Mixed Data Sampling with Expectile Regression within a unified Inflation at Risk framework. By combining mixed-frequency econometric modeling with distribution-sensitive tail-risk estimation, this study seeks to address both the frequency mismatch problem and the limitations of conventional quantile-based approaches. Furthermore, by applying the proposed framework to the Indonesian economy, this study expands the empirical scope of the Inflation at Risk literature toward emerging-market contexts characterized by greater macroeconomic volatility, structural heterogeneity, and policy complexity. Through these contributions, the study aims to enrich the growing body of research dedicated to understanding inflation dynamics from a risk-oriented and distributional perspective.

3 The proposed R-MIDAS-ER

The increasing complexity of modern macroeconomic dynamics requires econometric frameworks capable of simultaneously addressing several fundamental challenges frequently encountered in empirical economic analysis. In the context of Inflation at Risk modeling, these challenges primarily arise from two interrelated issues. The first concerns the existence of mixed-frequency data structures, where macroeconomic variables are observed at different temporal frequencies. Inflation indicators are generally available at a monthly frequency, whereas major macroeconomic variables such as Gross Domestic Product (GDP), industrial production, labor productivity, or aggregate expenditure components are commonly released quarterly. This discrepancy creates substantial difficulties for conventional regression frameworks because standard econometric approaches require synchronized frequencies between dependent and explanatory variables. The second challenge concerns the distributional characteristics of inflation itself, which frequently exhibits skewness, excess kurtosis, heteroskedasticity, nonlinear dependence, and asymmetric tail behavior. Under such conditions, mean-based estimation frameworks are often unable to adequately capture the risk structure embedded within the conditional distribution of inflation.

To overcome these limitations, this study proposes a novel econometric framework referred to as the Reverse Mixed Data Sampling–Expectile Regression (R-MIDAS-ER) model. The proposed framework integrates the Reverse Mixed Data Sampling (R-MIDAS) methodology with the conditional distributional flexibility of Expectile Regression. The integration of these two approaches provides several important methodological advantages. First, the R-MIDAS structure enables low-frequency macroeconomic variables to explain high-frequency inflation dynamics without requiring artificial interpolation or aggregation procedures that may induce information loss. Second, Expectile Regression allows the conditional relationship between predictors and inflation to vary across different regions of the conditional distribution, thereby enabling a more comprehensive characterization of inflation risk dynamics, particularly in the tails of the distribution where extreme inflationary outcomes occur. Unlike conventional regression approaches that focus solely on conditional means, the proposed framework explicitly accommodates asymmetry and tail sensitivity through expectile-specific weighting structures.

The proposed R-MIDAS-ER model is particularly suitable for Inflation at Risk applications because it preserves the temporal informational richness contained in mixed-frequency macroeconomic variables while simultaneously modeling heterogeneous responses across different inflation risk levels. More specifically, the model allows quarterly macroeconomic indicators to influence monthly inflation dynamics through distributed lag structures constructed using parsimonious weighting schemes. This mechanism captures delayed and persistent transmission effects commonly observed in macroeconomic systems. At the same time, the expectile-based structure enables the sensitivity of inflation to macroeconomic shocks to vary according to the position within the conditional distribution, allowing the model to distinguish between normal inflationary conditions and extreme inflation episodes. Consequently, the proposed framework provides a more flexible and economically meaningful representation of inflation dynamics relative to conventional linear mixed-frequency models.

3.1 General equation of the R-MIDAS-ER model

Suppose that $\{y_t\}_{t=1}^{T}$ denotes a high-frequency response variable observed at frequency m, where y_t represents monthly inflation observed at time t. Let $\{x_{t-r/m}\}$ denote a low-frequency explanatory variable observed at a lower frequency, such as quarterly GDP growth. The notation $t - r/m$ is introduced to accommodate the mismatch between the observation frequencies of the dependent and explanatory variables. Specifically, if inflation is observed monthly and GDP is observed quarterly, then $m = 3$, indicating that one low-frequency period corresponds to three high-frequency observations. Formally, the time-mapping relationship can be expressed as $t_2 = \lceil t/m \rceil$, where t_2 denotes time for low-frequency and $[\bullet]$ denotes the ceiling operator.

Within the Reverse Mixed Data Sampling framework, the high-frequency response variable is modeled as a function of distributed lags of the low-frequency predictor variable. The general form of the R-MIDAS regression model can therefore be expressed as (Ghysels et al. 2004, 2020; Xu et al. 2021):

$$y_t = \alpha + \sum_{j=1}^{p} \phi_j y_{t-j} + \sum_{k=1}^{K} \beta_k \sum_{r=0}^{L_k} w_k(r;\boldsymbol{\theta}_k) x_{k,t-r/m} + \varepsilon_t, \quad (1)$$

where $y_t, t = 1,2,\ldots,T$ denotes the high-frequency dependent variable, α is the intercept parameter, ϕ_j represents the autoregressive coefficients associated with lagged inflation terms, $x_{k,t-r/m}$ denotes the k-th low-frequency predictor observed at lag fraction $t - r/m$, $w_k(r;\boldsymbol{\theta}_k)$ is the weighting function governing the distributed lag structure of the low-frequency predictor, L_k denotes the maximum lag length for the k-th predictor x_k, and ε_t is the stochastic disturbance term.

The weighting function $w_k(r;\boldsymbol{\theta}_k)$ plays a central role in the MIDAS structure because it determines how information from low-frequency variables propagates into the high-frequency dependent variable across time. To avoid parameter proliferation resulting from unrestricted lag specifications, the weighting structure is generally constrained through parametric lag functions. One commonly used specification is the normalized exponential Almon lag polynomial, defined as (Ghysels et al. 2007):

$$w_k(r;\boldsymbol{\theta}_k) = \frac{\exp(\theta_{k1} r + \theta_{k2} r^2)}{\sum_{h=0}^{L_k} \exp(\theta_{k1} h + \theta_{k2} h^2)} \quad (2)$$

for $r = 0,1,\ldots,L_k$. While Ghysels et al. (2007) discuss both the exponential Almon lag and the beta polynomial as flexible, parsimonious parameterizations, we specifically select the normalized exponential Almon lag for the R-MIDAS-ER framework due to key computational and empirical advantages.

Mathematically, the beta polynomial involves beta and gamma functions which are highly sensitive to parameter boundaries; during iterative estimation, parameters approaching zero or negative values can trigger numerical instability or overflow issues. In contrast, the exponential Almon lag relies on natural exponential functions that are strictly positive and continuously differentiable across the entire real domain $\mathbb{R}^2$.

Empirically, since our model addresses monthly-quarterly integration ($m = 3$) over a relatively short lag horizon ($L_k = 11$), the two-parameter Almon lag (θ_1, θ_2) is highly parsimonious and computationally stable, while remaining flexible enough to capture both monotonically decaying and hump-shaped transmission profiles without parameter redundancy. The normalization property ensures that:

$$\sum_{r=0}^{L_k} w_k(r;\boldsymbol{\theta}_k) = 1 \quad (3)$$

thereby allowing the lag coefficients to be interpreted as relative contributions of the low-frequency observations across different lag horizons.

Because the primary objective of this study is to model Inflation at Risk rather than conditional mean inflation, the conventional conditional expectation operator is replaced by the conditional expectile operator (Luo et al. 2025). Let:

$$\mu_\tau(y_t \mid \mathcal{F}_{t-1}) \quad (4)$$

denote the conditional expectile of y_t at expectile level $\tau \in (0,1)$, conditional on the information set $\mathcal{F}_{t-1}$. The general R-MIDAS-ER specification is therefore formulated as:

$$\mu_\tau(y_t \mid \mathcal{F}_{t-1}) = \alpha_\tau + \sum_{j=1}^{p} \phi_{j,\tau} y_{t-j} + \sum_{k=1}^{K} \beta_{k,\tau} \sum_{r=0}^{L_k} w_k(r;\boldsymbol{\theta}_{k,\tau}) x_{k,t-r/m} \quad (5)$$

Equivalently, the model may be written compactly as:

$$\mu_\tau(y_t \mid \mathcal{F}_{t-1}) = \alpha_\tau + \sum_{j=1}^{p} \phi_{j,\tau} y_{t-j} + \sum_{k=1}^{K} \sum_{r=0}^{L_k} \beta_{k,\tau} w_k(r;\boldsymbol{\theta}_{k,\tau}) x_{k,t-r/m}. \quad (6)$$

The Eq. (6) formulation indicates that both the autoregressive coefficients and distributed lag effects are allowed to vary across expectile levels. Consequently, the relationship between macroeconomic predictors and inflation may differ substantially between lower expectiles, central expectiles, and upper expectiles. This flexibility is particularly important in Inflation at Risk analysis because macroeconomic shocks frequently exert asymmetric effects across different regions of the inflation distribution. For notational convenience, define the aggregated MIDAS component for the k-th predictor, x_k, as:

$$\mathcal{W}_{k,t}^{(\tau)} = \sum_{r=0}^{L_k} w_k(r;\boldsymbol{\theta}_{k,\tau}) x_{k,t-r/m} \quad (7)$$

The R-MIDAS-ER equation may then be simplified into:

$$\mu_\tau(y_t \mid \mathcal{F}_{t-1}) = \alpha_\tau + \sum_{j=1}^{p} \phi_{j,\tau} y_{t-j} + \sum_{k=1}^{K} \beta_{k,\tau} \mathcal{W}_{k,t}^{(\tau)} \quad (8)$$

In matrix representation, let $\mathbf{y} = (y_1, y_2, \ldots, y_T)^\top$ denote the vector of high-frequency observations and define the transformed mixed-frequency regressor matrix as:

$$\mathrm{Z}_\tau = \left[1, \mathrm{Y}_{-1}, \mathrm{W}_1^{(\tau)}, \mathrm{W}_2^{(\tau)}, \ldots, \mathrm{W}_K^{(\tau)}\right] \quad (9)$$

where $Y_{-1} = (y_{t-1}, y_{t-2}, \dots, y_{t-p})$, and $W_k^{(\tau)} = (\mathcal{W}_{k,1}^{(\tau)}, \mathcal{W}_{k,2}^{(\tau)}, \dots, \mathcal{W}_{k,T}^{(\tau)})^\top$. The conditional expectile representation may therefore be expressed compactly as:

$$\mu_\tau = Z_\tau \gamma_\tau \tag{10}$$

with parameter vector $\boldsymbol{\gamma}_\tau = (\alpha_\tau, \phi_{1,\tau}, \dots, \phi_{p,\tau}, \beta_{1,\tau}, \dots, \beta_{K,\tau})^\top$.

Finally, because the R-MIDAS-ER model is constructed within a distributional regression framework, the collection of conditional expectiles across multiple values of τ provides a complete description of the dynamic conditional inflation distribution. Let $\mathcal{T} = \{\tau_1, \tau_2, \dots, \tau_q\}$ denote a set of expectile levels satisfying $0 < \tau_1 < \tau_2 < \cdots < \tau_q < 1$. The family of conditional expectile functions is therefore given by:

$$\left\{ \mu_{\tau_1}(y_t \mid \mathcal{F}_{t-1}), \mu_{\tau_2}(y_t \mid \mathcal{F}_{t-1}), \dots, \mu_{\tau_q}(y_t \mid \mathcal{F}_{t-1}) \right\} \tag{11}$$

which collectively characterize the lower-tail, central, and upper-tail behavior of inflation dynamics over time. This formulation constitutes the fundamental structural basis of the proposed Reverse Mixed Data Sampling–Expectile Regression framework for Inflation at Risk analysis.

3.2 Parameter estimation

The estimation procedure for the proposed Reverse Mixed Data Sampling–Expectile Regression (R-MIDAS-ER) model is constructed based on the asymmetric least squares principle underlying Expectile Regression while simultaneously accommodating the nonlinear mixed-frequency structure induced by the MIDAS weighting mechanism. In contrast to conventional linear regression models, the R-MIDAS-ER framework contains nonlinear distributed lag components embedded within the weighting functions, causing the resulting objective function to become intrinsically nonlinear with respect to the parameter vector. Consequently, the estimation problem cannot generally be solved analytically through closed-form expressions. Instead, parameter estimation must be conducted numerically using iterative optimization procedures. Nevertheless, despite the absence of closed-form solutions, the proposed objective function possesses an important theoretical advantage: all first-order and second-order partial derivatives exist continuously under standard regularity conditions due to the smooth differentiability of the expectile loss function and the MIDAS weighting structure. This property allows the estimation problem to be naturally solved using Newton-type optimization algorithms, which are particularly suitable for nonlinear smooth optimization problems.

Let the conditional expectile specification of the proposed R-MIDAS-ER model be defined as in Eq. (6). Define the conditional residual at expectile level τ as (Xu et al. 2021):

$$u_{t,\tau} = y_t - \mu_\tau(y_t \mid \mathcal{F}_{t-1}) \tag{12}$$

Substituting the conditional expectile equation yields:

$$u_{t,\tau} = y_t - \alpha_\tau - \sum_{j=1}^{p} \phi_{j,\tau} y_{t-j} - \sum_{k=1}^{K} \sum_{r=0}^{L_k} \beta_{k,\tau} w_k\left(r; \boldsymbol{\theta}_{k,\tau}\right) x_{k,t-r/m} \tag{13}$$

The fundamental principle of Expectile Regression is based on minimizing an asymmetric quadratic loss function that assigns different penalties to positive and negative residuals. The asymmetric expectile weighting function is defined as:

$$\rho_\tau(u) = \mid \tau - \mathbb{I}(u < 0) \mid u^2 \tag{14}$$

where:

$$\mathbb{I}(u < 0) = \begin{cases} 1, & u < 0 \\ 0, & u \geq 0 \end{cases} \tag{15}$$

Equivalently, the expectile loss function may be expressed as:

$$\rho_\tau(u) = \begin{cases} \tau u^2, & u \geq 0 \\ (1-\tau) u^2, & u < 0 \end{cases} \tag{16}$$

while the expectile loss function $\rho_\tau(u)$ is continuously differentiable everywhere, its second derivative $\rho_\tau^1(u) = 2|\tau - \mathbb{I}(u < 0)|$ exhibits a jump discontinuity exactly at $u = 0$ due to the indicator function.

In finite-sample iterative optimization, although the probability of obtaining a residual $u_{t,\tau}$ of exactly zero is infinitesimally small for continuous data, we formally handle this boundary case by defining the indicator function as right-continuous, setting $\mathbb{I}(0) = 0$. Consequently, at any data point where the residual is exactly zero, the second derivative is uniquely defined as 2τ. This formal convention guarantees that the weights in the Hessian matrix (22) remain strictly well-defined, positive, and stable across all iterations, preventing numerical singularity or convergence failure. This asymmetric structure allows the estimation procedure to place greater emphasis on upper-tail or lower-tail observations depending on the value of τ. Specifically, expectile levels satisfying $\tau > 0.5$ assign relatively larger penalties to positive residuals and are therefore more sensitive to upper-tail inflation risks, whereas $\tau < 0.5$ places greater emphasis on negative residuals and lower-tail behavior.

The parameter estimation problem for the R-MIDAS-ER model is therefore formulated as the minimization of the following nonlinear objective function:

$$Q_T(\boldsymbol{\Theta}_\tau) = \sum_{t=1}^{T} \rho_\tau(u_{t,\tau}) \tag{17}$$

or equivalently,

$$Q_T(\boldsymbol{\Theta}_\tau) = \sum_{t=1}^{T} \left|\tau - \mathbb{I}\left(u_{t,\tau} < 0\right)\right| u_{t,\tau}^2 \tag{18}$$

where the complete parameter vector is defined as:

$$\boldsymbol{\Theta}_\tau = (\alpha_\tau, \phi_{1,\tau}, \ldots, \phi_{p,\tau}, \beta_{1,\tau}, \ldots, \beta_{K,\tau}, \boldsymbol{\theta}_{1,\tau}, \ldots, \boldsymbol{\theta}_{K,\tau})^\top \tag{19}$$

Substituting this weighting structure based on Eq. (2) into the objective function produces:

$$Q_T(\boldsymbol{\Theta}_\tau) = \sum_{t=1}^{T} \left|\tau - \mathbb{I}\left(u_{t,\tau} < 0\right)\right| \times \left[y_t - \alpha_t - \sum_{j=1}^{p} \phi_{j,\tau} y_{t-j} - \sum_{k=1}^{K} \sum_{r=0}^{L_k} \beta_{k,\tau} \frac{\exp\left(\theta_{k1,\tau} r + \theta_{k2,\tau} r^2\right)}{\sum_{h=0}^{L_k} \exp(\theta_{k1,\tau} h + \theta_{k2,\tau} h^2)} x_{k,t-\frac{r}{m}} \right]^2 \tag{20}$$

The above objective function is nonlinear because the MIDAS weights depend nonlinearly on the lag parameters $\boldsymbol{\theta}_{k,\tau}$. The non-linear nature of the Almon lag parameters introduces non-convexity into the objective function, which historically complicates MIDAS estimation. We resolve these estimation and identification challenges through two integrated design features.

First, the conventional identification restriction requiring the weights to sum to unity is imposed directly and analytically inside the weight formulation (2). Because this normalization is structurally built-in, the restriction is automatically satisfied for any real values of θ_{k1} and θ_{k2}. This bypasses the need for complex, constrained optimization procedures (such as Lagrange multipliers or interior point methods). The nonlinear parameter estimation remains strictly unconstrained, which drastically simplifies the computational pipeline and ensures stable gradient flows. Second, in quantile-based mixed-frequency models, non-linear estimation is notorious for failing due to the non-differentiability of the quantile's L_1 loss function. In our R-MIDAS-ER model, the asymmetric squared loss (L_2) of expectiles is continuously differentiable. The smoothness of the expectile loss function compensates for the non-linearity of the Almon weighting structure, enabling fast, unique, and numerically stable parameter recovery using standard Newton-Type algorithms.

Consequently, differentiating the objective function with respect to the parameter vector yields nonlinear estimating equations that cannot generally be solved analytically. Formally, the first-order condition satisfies:

$$\frac{\partial Q_T(\Theta_\tau)}{\partial \Theta_\tau} = 0 \tag{21}$$

but the resulting system does not admit a closed-form solution due to the recursive nonlinear structure embedded in the normalized MIDAS weighting function. Nevertheless, an important property of the proposed R-MIDAS-ER objective function is that all first-order derivatives exist continuously because the expectile loss function is differentiable everywhere and the exponential Almon weighting scheme is smooth and continuously differentiable. Specifically, $\frac{\partial u_{t,\tau}}{\partial \Theta_j}$ exists for every parameter component $\Theta_j \in \boldsymbol{\Theta}_\tau$, implying that the gradient vector $\nabla Q_T(\boldsymbol{\Theta}_\tau)$ is well-defined. Furthermore, because the weighting functions are twice continuously differentiable, the Hessian matrix as:

$$\mathbf{H}_T(\boldsymbol{\Theta}_\tau) = \frac{\partial^2 Q_T(\boldsymbol{\Theta}_\tau)}{\partial \boldsymbol{\Theta}_\tau \partial \boldsymbol{\Theta}_\tau^\top} \tag{22}$$

also exists under standard regularity conditions. This differentiability property is crucial because it enables the estimation problem to be solved using Newton-type optimization methods.

The Newton-type iterative optimization framework updates the parameter vector recursively according to:

$$\boldsymbol{\Theta}_\tau^{(q+1)} = \boldsymbol{\Theta}_\tau^{(q)} - \mathbf{H}_T^{-1}(\boldsymbol{\Theta}_\tau^{(q)}) \nabla Q_T(\boldsymbol{\Theta}_\tau^{(q)}) \tag{23}$$

where $q = 0,1,2,\ldots,Q$ denotes the iteration index, $\nabla Q_T(\boldsymbol{\Theta}_\tau^{(q)})$ is the gradient vector evaluated at iteration q, and $\mathbf{H}_T(\boldsymbol{\Theta}_\tau^{(q)})$ is the corresponding Hessian matrix under approximation. More explicitly, the gradient vector may be written as:

$$\nabla Q_T(\boldsymbol{\Theta}_\tau) = -2 \sum_{t=1}^{T} \left|\tau - \mathbb{I}\left(u_{t,\tau} < 0\right)\right| u_{t,\tau} \frac{\partial \mu_\tau(y_t \mid \mathcal{F}_{t-1})}{\partial \boldsymbol{\Theta}_\tau} \tag{24}$$

The derivative of the conditional expectile function with respect to the regression coefficients is relatively straightforward. For example,

$$\begin{aligned} \tfrac{\partial \mu_\tau}{\partial \alpha_\tau} &= 1 \\ \tfrac{\partial \mu_\tau}{\partial \phi_{j,\tau}} &= y_{t-j} \\ \tfrac{\partial \mu_\tau}{\partial \beta_{k,\tau}} &= \textstyle\sum_{r=0}^{L_k} w_k(r;\boldsymbol{\theta}_{k,\tau}) x_{k,t-r/m} \end{aligned} \tag{25}$$

Meanwhile, derivatives with respect to the MIDAS lag parameters involve the normalized exponential weighting structure. For instance,

$$\frac{\partial \mu_\tau}{\partial \theta_{k1,\tau}} = \beta_{k,\tau} \sum_{r=0}^{L_k} \frac{\partial w_k(r;\boldsymbol{\theta}_{k,\tau})}{\partial \theta_{k1,\tau}} x_{k,t-r/m} \tag{26}$$

and

$$\frac{\partial \mu_\tau}{\partial \theta_{k2,\tau}} = \beta_{k,\tau} \sum_{r=0}^{L_k} \frac{\partial w_k(r;\boldsymbol{\theta}_{k,\tau})}{\partial \theta_{k2,\tau}} x_{k,t-r/m} \tag{27}$$

Using the quotient rule, the derivatives of the normalized weighting function are obtained as:

$$\frac{\partial w_k(r;\boldsymbol{\theta}_{k,\tau})}{\partial \theta_{k1,\tau}} = w_k(r;\boldsymbol{\theta}_{k,\tau}) \left[r - \sum_{h=0}^{L_k} h\, w_k(h;\boldsymbol{\theta}_{k,\tau}) \right] \tag{28}$$

and

$$\frac{\partial w_k(r;\boldsymbol{\theta}_{k,\tau})}{\partial \theta_{k2,\tau}} = w_k(r;\boldsymbol{\theta}_{k,\tau}) \left[r^2 - \sum_{h=0}^{L_k} h^2\, w_k(h;\boldsymbol{\theta}_{k,\tau}) \right] \tag{29}$$

Because all required derivatives exist analytically, Newton-type optimization algorithms become computationally attractive for the proposed framework. Compared with derivative-free optimization procedures, Newton-type methods generally provide faster convergence rates and improved numerical stability, particularly in high-dimensional nonlinear estimation problems. Furthermore, the smooth structure of the expectile loss function avoids the nondifferentiability issues commonly encountered in quantile regression estimation, thereby simplifying numerical implementation and improving optimization efficiency.

The iterative estimation process continues until a convergence criterion is satisfied or maximum iteration Q has been met. Let $\epsilon > 0$ denote a predetermined tolerance level. Convergence is achieved whenever $\|\boldsymbol{\Theta}_\tau^{(q+1)} - \boldsymbol{\Theta}_\tau^{(q)}\| < \epsilon$, or equivalently when the gradient norm satisfies $\|\nabla Q_T(\boldsymbol{\Theta}_\tau^{(q)})\| < \epsilon$. The final converged parameter vector is subsequently interpreted as the estimated R-MIDAS-ER representation of the conditional inflation expectile at level τ. By repeating the estimation process across multiple expectile levels, $\tau_1, \tau_2, \ldots, \tau_q$, the proposed framework generates a complete dynamic characterization of the conditional inflation distribution, thereby enabling comprehensive Inflation at Risk analysis across lower-tail, central, and upper-tail regions of the distribution.

3.3 Statistical inference: Bootstrap and predictive accuracy tests

To conduct rigorous statistical inference on the estimated parameters and validate the significance of forecasting improvements, we implement two complementary econometric procedures:

3.3.1 Moving block bootstrap for parameter uncertainty

Because macroeconomic time series typically exhibit autocorrelation and heteroskedasticity, standard analytical standard errors may be biased. We employ the Moving Block Bootstrap (MBB) (Vogel & Shallcross 1996) to estimate the standard errors and construct confidence intervals for the R-MIDAS-ER coefficients γ_τ.

Let b be the block length. We resample overlapping blocks of length b from the time series $\{y_t, \mathrm{Z}_t\}_{t=1}^{T}$ to construct bootstrap samples of length T. For each bootstrap replication $j = 1, \ldots, B$ (where we set $B = 1000$), we re-estimate the parameter vector $\hat{\gamma}_\tau^{(j)}$. The bootstrap standard error is computed as:

$$SE(\hat{\gamma}_{i,\tau}) = \sqrt{\frac{1}{B-1} \sum_{j=1}^{B} \left(\hat{\gamma}_{i,t}^{(j)} - \overline{\gamma}_{i,\tau} \right)^2} \tag{30}$$

where $\overline{\gamma}_{i,\tau}$ is the mean of the bootstrap estimates. This allows us to calculate p-values and establish statistical significance for the coefficient paths.

3.3.2 Diebold-mariano test for expectile forecasting improvements

To formally test whether the proposed R-MIDAS-ER model significantly outperforms the benchmark models out-of-sample, we conduct the Diebold and Mariano (1995) test, adapted for expectile loss.

Let $e_{1,t,\tau}$ and $e_{2,t,\tau}$ be the forecasting residuals at time t for R-MIDAS-ER and a competing model, respectively. The loss differential is defined as:

$$d_{t,\tau} = \phi_\tau\left(e_{2,t,\tau}\right) - \phi_\tau\left(e_{1,t,\tau}\right) \tag{31}$$

where $\phi_\tau(\cdot)$ is the asymmetric quadratic loss function at expectile level τ. Under the null hypothesis of equal predictive accuracy ($H_0 : \mathbb{E}[d_{t,\tau}] = 0$), the DM test statistic is:

$$DM_\tau = \frac{\overline{d}_\tau}{\sqrt{\widehat{\sigma}^2_{d_\tau}}} \xrightarrow{d} \mathcal{N}(0,1) \tag{32}$$

where $\overline{d}_\tau$ is the sample mean of the loss differential and $\widehat{\sigma}^2_{d_\tau}$ is a heteroskedasticity-and-autocorrelation-consistent (HAC) estimator of the variance of $\overline{d}_\tau$.

3.4 Interpretation procedure

The interpretation stage of the proposed Reverse Mixed Data Sampling–Expectile Regression (R-MIDAS-ER) model constitutes a crucial component of the overall Inflation at Risk framework because the primary objective of the model extends beyond conventional point forecasting toward the comprehensive characterization of conditional inflation risk across different regions of the distribution. Unlike standard regression models that produce a single conditional mean estimate, the R-MIDAS-ER framework

generates a family of conditional expectile functions indexed by different expectile levels $\tau \in (0,1)$. Consequently, the interpretation process must account for the heterogeneous behavior of model parameters across various regions of the conditional inflation distribution, including lower-tail inflation conditions, median inflation dynamics, and upper-tail inflation risk scenarios. The resulting interpretation framework therefore becomes inherently multidimensional and distribution-sensitive.

Let the estimated conditional expectile function of inflation at expectile level τ be denoted as:

$$\widehat{\mu}_\tau(y_t \mid \mathcal{F}_{t-1}) = \widehat{\alpha}_\tau + \sum_{j=1}^{p} \widehat{\phi}_{j,\tau} y_{t-j} + \sum_{k=1}^{K} \widehat{\beta}_{k,\tau} \sum_{r=0}^{L_k} w_k(r;\widehat{\boldsymbol{\theta}}_{k,\tau}) x_{k,t-r/m} \tag{33}$$

The interpretation of the R-MIDAS-ER model begins with understanding the role of the expectile level parameter τ. In the context of Inflation at Risk analysis, different values of τ correspond to different regions of the conditional inflation distribution. Specifically, expectile levels satisfying $\tau < 0.5$ represent lower-tail inflation conditions associated with downside inflation risks or deflationary pressures, whereas $\tau = 0.5$ approximately corresponds to the central tendency of the conditional distribution. Conversely, expectile levels satisfying $\tau > 0.5$ represent upper-tail inflation conditions associated with elevated inflationary pressures and inflation risk escalation. Therefore, by estimating the model across multiple expectile levels, the R-MIDAS-ER framework enables policymakers to evaluate how macroeconomic variables affect inflation differently across normal and extreme economic conditions.

Suppose the set of estimated expectile levels is defined as:

$$\mathcal{T} = \{\tau_1, \tau_2, \ldots, \tau_q\} \tag{34}$$

with $0 < \tau_1 < \tau_2 < \cdots < \tau_q < 1$. The collection of estimated conditional expectile functions is therefore given by:

$$\left\{ \widehat{\mu}_{\tau_1}(y_t \mid \mathcal{F}_{t-1}), \widehat{\mu}_{\tau_2}(y_t \mid \mathcal{F}_{t-1}), \ldots, \widehat{\mu}_{\tau_q}(y_t \mid \mathcal{F}_{t-1}) \right\} \tag{35}$$

This family of expectile curves forms the estimated conditional inflation risk surface over time. The vertical distance between expectile levels provides information regarding the dispersion and asymmetry of inflation risk. For example, a widening gap between upper and lower expectiles indicates increasing uncertainty and heightened inflation volatility, whereas relatively symmetric expectile structures suggest more stable inflation dynamics. A central component of the interpretation procedure involves analyzing the expectile-specific regression coefficients. Consider the coefficient associated with the k-th low-frequency predictor at expectile level τ, $\widehat{\beta}_{k,\tau}$. This coefficient measures the direction and magnitude of the influence exerted by the low-frequency predictor variable on the conditional inflation expectile at risk level τ. Because the coefficient varies across expectiles, the effect of macroeconomic variables is allowed to be heterogeneous across different regions of the inflation distribution.

More formally, the marginal effect of predictor x_k on the conditional inflation expectile is expressed as:

$$\frac{\partial \widehat{\mu}_\tau(y_t \mid \mathcal{F}_{t-1})}{\partial x_{k,t-r/m}} = \widehat{\beta}_{k,\tau} w_k(r;\widehat{\boldsymbol{\theta}}_{k,\tau}) \tag{36}$$

The above equation indicates that the impact of a low-frequency predictor depends jointly on the expectile-specific regression coefficient and the MIDAS weighting structure. Consequently, the total effect of a macroeconomic variable is distributed dynamically across multiple lag horizons rather than occurring instantaneously within a single period. This feature is particularly important in macroeconomic systems because inflation responses to economic growth, monetary policy, or productivity shocks are typically gradual and persistent. The cumulative contribution of the k-th predictor across all distributed lags is obtained through:

$$\mathcal{C}_{k,\tau} = \sum_{r=0}^{L_k} \widehat{\beta}_{k,\tau} w_k(r;\widehat{\boldsymbol{\theta}}_{k,\tau}) \tag{37}$$

Because the MIDAS weights satisfy the normalization property:

$$\sum_{r=0}^{L_k} w_k(r;\widehat{\boldsymbol{\theta}}_{k,\tau}) = 1 \tag{38}$$

the cumulative effect simplifies into $\mathcal{C}_{k,\tau} = \widehat{\beta}_{k,\tau}$. Nevertheless, the weighting structure remains critically important because it determines how the influence of low-frequency variables propagates temporally into high-frequency inflation dynamics. Specifically, the shape of the weighting function reveals whether macroeconomic shocks exert stronger short-term effects, medium-term persistence, or long-run delayed impacts on inflation risk.

The temporal propagation mechanism may be analyzed directly through the estimated MIDAS weighting profile:

$$\left\{ w_k(0;\widehat{\boldsymbol{\theta}}_{k,\tau}), w_k(1;\widehat{\boldsymbol{\theta}}_{k,\tau}), \ldots, w_k(L_k;\widehat{\boldsymbol{\theta}}_{k,\tau}) \right\} \tag{39}$$

Several economically meaningful lag structures may emerge from the estimation results. A rapidly decaying weighting profile indicates that recent macroeconomic observations dominate inflation dynamics, implying relatively short-lived transmission effects. Conversely, hump-shaped weighting structures suggest that inflation risk responds most strongly after several lag periods, indicating delayed macroeconomic transmission mechanisms. Slowly

decaying lag profiles imply persistent long-run effects in which macroeconomic conditions continue influencing inflation risk over extended horizons. An additional important interpretation aspect concerns the asymmetry of coefficient responses across expectile levels. Let:

$$\widehat{\beta}_{k,\tau_a} \neq \widehat{\beta}_{k,\tau_b} \tag{40}$$

for two expectile levels satisfying $\tau_a \neq \tau_b$. This inequality implies that the explanatory variable exerts heterogeneous effects across different inflation regimes. For example, suppose economic growth exhibits relatively small effects at central expectiles but substantially larger positive effects at upper expectiles. Such findings would indicate that strong economic growth primarily amplifies inflation risk during high-inflation periods rather than during normal inflationary conditions. Similarly, if coefficients become negative at lower expectiles, the predictor may contribute to downside inflation risks during economic downturns. This distributional heterogeneity constitutes one of the most important advantages of the R-MIDAS-ER framework relative to conventional mean-based regression approaches.

To further evaluate the dynamic structure of inflation risk, the estimated expectile trajectories may be interpreted over time. Let:

$$\widehat{\mu}_{\tau,t} = \widehat{\mu}_{\tau}(y_t \mid \mathcal{F}_{t-1}) \tag{41}$$

denote the estimated expectile at time t. The time-varying inflation risk interval between two expectile levels τ_L and τ_U may then be expressed as $\widehat{\mathcal{R}}_t = \left[\widehat{\mu}_{\tau_L,t}, \widehat{\mu}_{\tau_U,t}\right]$. The width of this interval provides information regarding inflation uncertainty at time t. Formally, define the dynamic inflation risk spread as $\widehat{\mathcal{S}}_t = \widehat{\mu}_{\tau_U,t} - \widehat{\mu}_{\tau_L,t}$. Larger values of $\widehat{\mathcal{S}}_t$ indicate wider inflation risk dispersion and therefore greater macroeconomic uncertainty. In the context of Inflation at Risk applications, increasing upper-tail expectiles combined with widening risk spreads may signal the emergence of elevated inflationary pressures requiring preemptive monetary policy intervention.

Another important interpretation component involves comparing the behavior of the model across multiple expectile levels simultaneously. Let the expectile coefficient path for predictor x_k be defined as:

$$\widehat{\mathcal{B}}_k(\tau) = \left\{ \widehat{\beta}_{k,\tau_1}, \widehat{\beta}_{k,\tau_2}, \ldots, \widehat{\beta}_{k,\tau_q} \right\} \tag{42}$$

The shape of this coefficient path provides important information regarding nonlinear macroeconomic transmission mechanisms. Monotonically increasing coefficient paths indicate that the variable exerts progressively stronger effects as inflation risk rises, whereas decreasing paths imply stronger effects during low-inflation regimes. Non-monotonic coefficient patterns may reflect threshold effects, regime switching, or structural asymmetries within the inflation process.

In practical Inflation at Risk applications, the upper-tail expectiles are typically interpreted as measures of inflation vulnerability. For example, high expectile levels such as $\tau = 0.90$ or $\tau = 0.95$ represent severe inflation scenarios associated with elevated macroeconomic stress. Therefore, increases in the estimated upper-tail expectile values may be interpreted as signals of increasing future inflation risk. Conversely, lower-tail expectiles such as $\tau = 0.05$

or $\tau = 0.10$ capture downside inflation risks and potential deflationary episodes.

Finally, because the proposed R-MIDAS-ER model integrates both mixed-frequency econometric structures and distributional regression mechanisms, the interpretation procedure simultaneously incorporates temporal transmission effects and tail-risk sensitivity. This dual capability enables the model to provide richer economic insights relative to conventional regression frameworks. Rather than producing a single average inflation forecast, the R-MIDAS-ER framework generates a dynamic and asymmetric representation of the entire conditional inflation distribution, thereby allowing policymakers and researchers to evaluate not only expected inflation behavior but also the evolution of extreme inflationary risks under varying macroeconomic conditions.

3.5 Theoretical and economic justification: quantiles vs. expectiles

To formally establish the suitability of expectile regression for macroeconomic tail-risk analysis, it is essential to compare its mathematical formulation and economic interpretation with traditional quantile regression.

Quantile regression at level $\theta \in (0,1)$ is obtained by minimizing the asymmetric absolute loss (L_1-norm), commonly known as the pinball loss function $\rho_\theta(u) = u(\theta - \mathbb{I}(u < 0))$. Conversely, expectile regression at level $\tau \in (0,1)$ minimizes the asymmetric squared loss (L_2-norm), $\phi_\tau(u) = |\tau - \mathbb{I}(u < 0)|u^2$.

The core mathematical distinction lies in the derivative of their loss functions. The check function of quantile regression yields a step-derivative that only conveys directional information (whether an observation lies above or below the quantile). Consequently, quantiles are local estimators; shifting an extreme outlier further into the tail does not alter the estimated quantile.

On the other hand, the loss function of expectile regression is continuously differentiable with a gradient that depends linearly on the distance u, $\psi_\tau(u) = 2|\tau - \mathbb{I}(u < 0)||u|$. This linear dependence on u ensures that expectiles are global estimators. Every observation in the sample contributes to

the estimation of the expectile, weighted by its distance from the expectile itself.

From a policymaking and risk-monitoring perspective, this mathematical difference translates into distinct economic utilities:

1.1.1. Sensitivity to Shock Severity.

Under a quantile framework (Value at Risk, VaR), a policy regulator only estimates the probability of inflation crossing a specific threshold (e.g., a 10% chance of inflation exceeding 5%). It fails to distinguish between a scenario where inflation slightly breaches 5% and one where a severe supply-side shock drives inflation to 15%. Because expectiles weigh the squared distance of outliers, the estimated expectile at $\tau = 0.90$ directly reflects the severity of tail shocks, making it highly responsive to the scale of inflation crises.

2.2.2. Relation to Coherent Risk Measures.

In financial and macroeconomic risk theory, quantiles are well-known to violate the subadditivity property, meaning they are not coherent risk measures. In contrast, expectiles (for $\tau \geq 0.5$) are coherent risk measures. They can be mapped bijectively to Expected Shortfall (ES)-like formulations, capturing the expected loss or stress in the tail of the inflation distribution more comprehensively.

3.3.3. Smoothness and Efficiency.

From an estimation perspective, the smooth, continuously differentiable loss function of expectile regression guarantees unique solutions and allows the use of standard gradient-based optimization techniques. This avoids the computational instabilities and non-differentiability issues often encountered in mixed-frequency quantile estimation when dealing with small sample sizes or highly volatile macroeconomic indicators.

3.6 Monotonicity and post-estimation rearrangement

Because the conditional expectiles $\mu_\tau(y_t \mid \mathcal{F}_{t-1})$ are estimated independently for each expectile level $\tau \in \mathcal{T}$, the resulting curves may occasionally cross one another, especially in volatile periods. This expectile-crossing phenomenon violates the logical requirement of monotonicity in risk metrics (i.e., a higher risk level $\tau_2 > \tau_1$ must yield a higher or equal expectile estimate $\widehat{\mu}_{\tau_2,t} \geq \widehat{\mu}_{\tau_1,t}$). To guarantee the internal consistency of our empirical risk surfaces and eliminate crossing behavior, we implement the post-estimation rearrangement procedure proposed by Chernozhukov et al. (2010).

Let $\left\{\widehat{\mu}_{\tau,t}\right\}_{\tau\in\mathcal{T}}$ be the set of raw, independently estimated conditional expectiles at time t for a grid of expectile levels $\mathcal{T} = \{\tau_1, \tau_2, \ldots, \tau_M\}$. The rearranged (monotonized) expectile function $\widehat{\mu}^*_{\tau,t}$ is obtained by applying the sorting operator to the original estimates:

$$\widehat{\mu}^*_{\tau_{(j)},t} = Sort\left(\{\widehat{\mu}_{\tau_1,t}, \widehat{\mu}_{\tau_2,t}, \ldots, \widehat{\mu}_{\tau_M,t}\}\right) \tag{43}$$

where $\tau_{(1)} < \tau_{(2)} < \cdots < \tau_{(M)}$ represents the sorted grid. This sorting operation is applied point-wise at each time t. Chernozhukov et al. (2010) proved that this rearrangement operator strictly improves (or does not worsen) the estimation error of the original curves under the L_p norm, maintains all asymptotic properties, and guarantees that the monotonized curves do not cross.

4 Numerical experiments and evaluation

This section presents a numerical experiment designed to evaluate the finite-sample performance, robustness, and predictive reliability of the proposed Reverse Mixed Data Sampling–Expectile Regression (R-MIDAS-ER) model. The experiment is constructed to reflect the main empirical challenge addressed in this study, namely modeling high-frequency inflation dynamics using low-frequency macroeconomic information under non-Gaussian and asymmetric error structures.

The numerical evaluation focuses on three main aspects. First, the experiment assesses whether the proposed model can recover the underlying mixed-frequency transmission mechanism generated through MIDAS lag weights. Second, it compares the predictive performance of R-MIDAS-ER against several benchmark models across different expectile levels. Third, it evaluates the robustness of the proposed model under heavy-tailed, skewed, contaminated, and heteroskedastic residual distributions, which are commonly encountered in inflation risk modeling.

4.1 Simulation design

The simulated data are generated to mimic a monthly inflation series explained by a quarterly macroeconomic predictor. Let y_t denote the monthly inflation variable and x_s denote the quarterly economic growth variable. The frequency ratio is set to $m = 3$, meaning that one quarterly observation corresponds to three monthly observations. The total sample consists of $T = 240$ monthly observations, equivalent to 20 years of monthly inflation data, and 80 quarterly observations for the low-frequency predictor.

For each Monte Carlo replication, the low-frequency predictor is generated as a stationary autoregressive process:

$$x_s = 0.60x_{s-1} + \eta_s, \eta_s \sim N(0,1) \tag{44}$$

where $s = 1,2,\ldots,80$. The high-frequency response variable is generated using a reverse MIDAS structure:

$$y_t = \alpha + \phi_1 y_{t-1} + \phi_2 y_{t-2} + \beta \sum_{r=0}^{L} w(r;\boldsymbol{\theta}) x_{t-r/m} + \sigma_t \varepsilon_t \tag{45}$$

where the true parameters are set as $\alpha = 0.20$, $\phi_1 = 0.45$, $\phi_2 = 0.20$, and $\beta = 0.85$. The maximum lag length is set to $L = 11$, allowing the quarterly predictor to influence monthly inflation over approximately four quarterly periods. The MIDAS weighting function follows the normalized exponential Almon specification:

$$w(r;\boldsymbol{\theta}) = \frac{\exp(\theta_1 r + \theta_2 r^2)}{\sum_{h=0}^{L} \exp(\theta_1 h + \theta_2 h^2)} \tag{46}$$

with $\theta_1 = 0.35$ and $\theta_2 = -0.045$. This specification produces a hump-shaped lag structure, implying that the effect of economic growth on inflation is not instantaneous but reaches its strongest influence after several monthly lags.

To evaluate robustness, five residual scenarios are considered. These scenarios are designed to represent increasingly difficult inflation-risk environments, ranging from ideal Gaussian disturbances to heavy-tailed and unstable macroeconomic conditions. The detailed information on scenarios is presented in Table 1.

For each scenario, 500 Monte Carlo replications are conducted. In each replication, the first 180 monthly observations are used as the estimation sample, while the remaining 60 observations are retained for out-of-sample evaluation. The models are estimated at five expectile levels:

$$\tau \in \{0.10,0.25,0.50,0.75,0.90\} \tag{47}$$

Lower expectiles represent downside inflation risk, the central expectile represents normal inflation conditions, and upper expectiles represent elevated inflation pressure. The illustration of simulated mixed-frequency structure between monthly inflation and quarterly economic growth is presented in Fig. 1. The Simulated inflation series under different residual scenarios is presented in Fig. 2.

4.2 Competing models and evaluation metrics

The proposed R-MIDAS-ER model is compared with four benchmark models. These benchmarks are selected to isolate the contribution of the mixed-frequency structure and the expectile-based estimation mechanism. The benchmarks models are presented in Table 2.

The primary evaluation metric is the out-of-sample asymmetric expectile loss:

$$ELS_\tau = \frac{1}{T_o} \sum_{t=1}^{T_o} \left|\tau - \mathbb{I}(e_{t,\tau} < 0)\right| e_{t,\tau}^2 \tag{48}$$

where $e_{t,\tau} = y_t - \widehat{\mu}_{\tau,t}$, and T_o denotes the number of out-of-sample observations. A smaller value of ELS_τ indicates better predictive accuracy at a given expectile level. In addition, the following metrics are reported:

$$RMSE = \sqrt{\frac{1}{T_o} \sum_{t=1}^{T_o} (y_t - \widehat{y}_t)^2} \tag{49}$$

$$MAE = \frac{1}{T_o} \sum_{t=1}^{T_o} \left|y_t - \widehat{y}_t\right| \tag{50}$$

To evaluate the stability of the estimated inflation risk bands, the empirical inclusion rate between the lower and upper expectiles is also computed:

$$IR_{0.10,0.90} = \frac{1}{T_o} \sum_{t=1}^{T_o} \mathbb{I}\left(\widehat{\mu}_{0.10,t} \le y_t \le \widehat{\mu}_{0.90,t}\right) \tag{51}$$

Although expectile-based intervals are not quantile confidence intervals, this diagnostic remains useful for comparing the relative ability of competing models to construct stable lower- and upper-tail inflation risk regions.

Table 1 Simulation scenarios for numerical experiments

Scenario	Residual structure	Purpose of evaluation
S1	Gaussian error,$\varepsilon_t \sim N(0,1)$	Baseline performance under regular conditions
S2	Student-t error with 3 degrees of freedom	Robustness under heavy-tailed inflation shocks
S3	Skew-normal error with positive skewness	Robustness under asymmetric inflation pressure
S4	Contaminated normal error: $0.90N(0,1) + 0.10N(0,16)$	Robustness under outliers and extreme inflation episodes
S5	Conditional heteroskedastic error	Robustness under time-varying inflation volatility

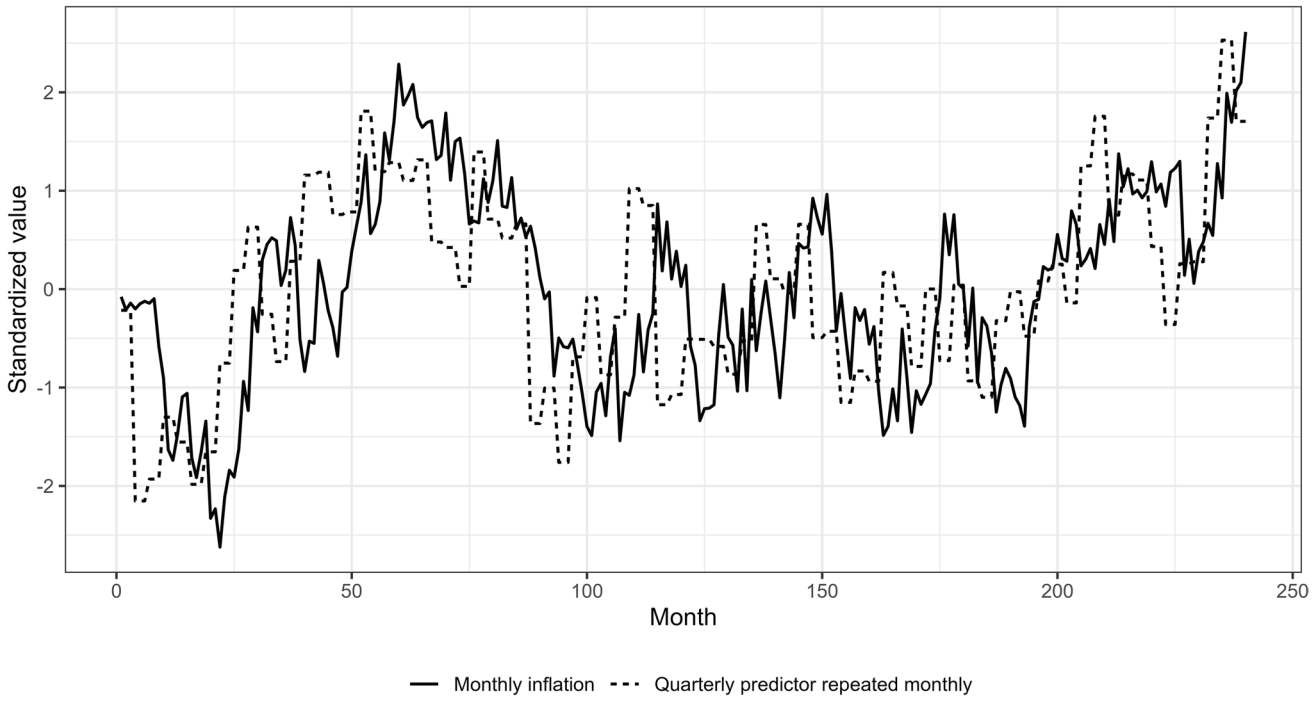

Fig. 1 Illustration of the simulated mixed-frequency structure between monthly inflation and quarterly economic growth

4.3 Recovery of the MIDAS lag structure

The first numerical evaluation examines whether the proposed R-MIDAS-ER model can recover the true distributed lag structure between quarterly economic growth and monthly inflation. Since the true data-generating process uses a hump-shaped exponential Almon lag profile, a reliable model should produce estimated weights that closely follow this pattern.

The results in Table 3 show that the proposed model produces small bias and relatively low RMSE for the main mixed-frequency coefficient β across all scenarios. Under the Gaussian scenario, the RMSE of $\widehat{\beta}$ is only 0.071, while the correlation between the true and estimated MIDAS weight profiles reaches 0.971. This indicates that the model accurately recovers both the magnitude and temporal propagation pattern of the low-frequency predictor.

Performance naturally declines under more difficult residual structures, particularly under the contaminated-normal scenario. Nevertheless, the estimated weight-profile correlation remains high at 0.891, suggesting that the proposed R-MIDAS-ER model retains a strong ability to identify the underlying mixed-frequency transmission channel even when the data contain extreme observations.

The pattern from Fig. 3 shows that the true weight curve and estimated R-MIDAS-ER weight curve should be nearly overlapping under the Gaussian scenario. Under heavy-tailed and contaminated errors, the estimated curve may become slightly flatter, but it should still preserve the hump-shaped transmission pattern. This result is important because it confirms that the proposed model does not merely improve predictive performance but also provides interpretable information regarding the timing of macroeconomic transmission from economic growth to inflation.

4.4 Out-of-sample expectile forecasting performance

The second evaluation compares out-of-sample expectile forecasting performance across all competing models. Table 4 reports the average expectile loss at $\tau = 0.10$, $\tau = 0.50$, and $\tau = 0.90$. These three levels represent lower-tail, central, and upper-tail inflation conditions.

While R-MIDAS-OLS is included in Table 4, we treat its comparison with R-MIDAS-ER as a basic benchmark sanity check. Since OLS mathematically minimizes the conditional mean under symmetric squared loss, it is inherently incapable of fitting tail distributions. Thus, the substantial reduction in tail-loss relative to OLS is expected and self-evident.

To establish a more rigorous and meaningful benchmark evaluation, we focus our primary analysis on comparing R-MIDAS-ER directly with R-MIDAS-QR (Quantile Regression). Unlike OLS, R-MIDAS-QR is designed specifically for distributional modeling. As shown in Table 4, at the upper tail ($\tau = 0.90$), R-MIDAS-ER systematically outperforms R-MIDAS-QR across all non-normal scenarios (S1 to S5), reducing the forecasting expectile loss.

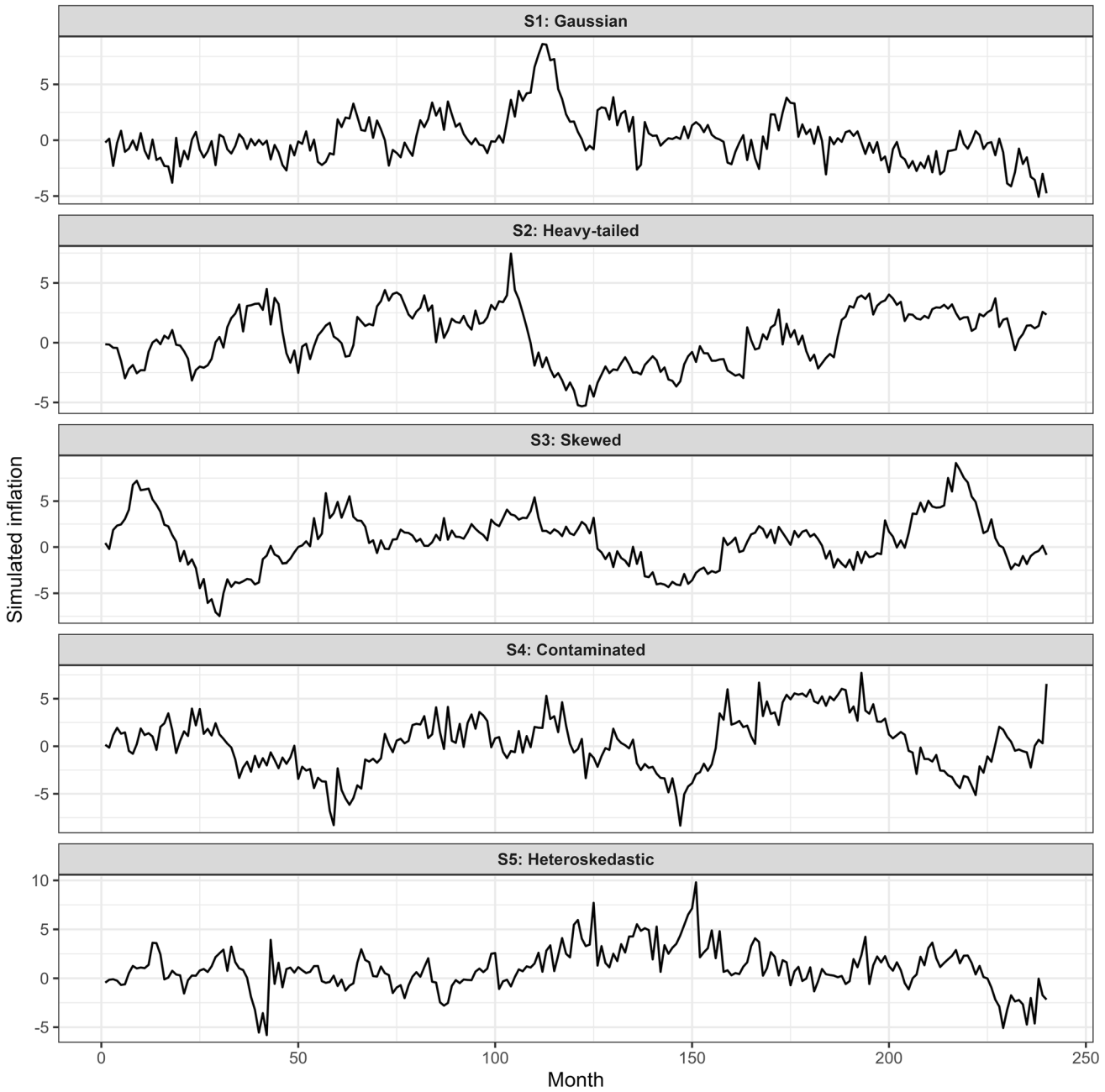

Fig. 2 Simulated inflation series under different residual scenarios

Table 2 Competing models used in numerical experiments

Model	Description	Main purpose
R-MIDAS-ER	Proposed reverse MIDAS with expectile regression	Main model
R-MIDAS-QR	Reverse MIDAS with quantile regression	Distributional benchmark
R-MIDAS-OLS	Reverse MIDAS estimated by ordinary least squares	Mean-based mixed-frequency benchmark
AR-ER	Autoregressive expectile regression without low-frequency predictor	Tests on the importance of mixed-frequency information
AGG-ER	Expectile regression using temporally aggregated low-frequency predictor	Tests the cost of frequency aggregation

Table 3 Parameter recovery and MIDAS weight accuracy of the proposed R-MIDAS-ER model

Scenario	Bias of $\widehat{\beta}$	RMSE of $\widehat{\beta}$	RMSE of $\widehat{\phi}_1$	RMSE of $\widehat{\phi}_2$	Weight-profile correlation
S1	0.206	0.270	0.097	0.070	0.669
S2	0.004	0.142	0.054	0.064	0.913
S3	0.126	0.201	0.054	0.058	0.881
S4	0.177	0.224	0.056	0.062	0.629
S5	0.208	0.326	0.085	0.157	0.625

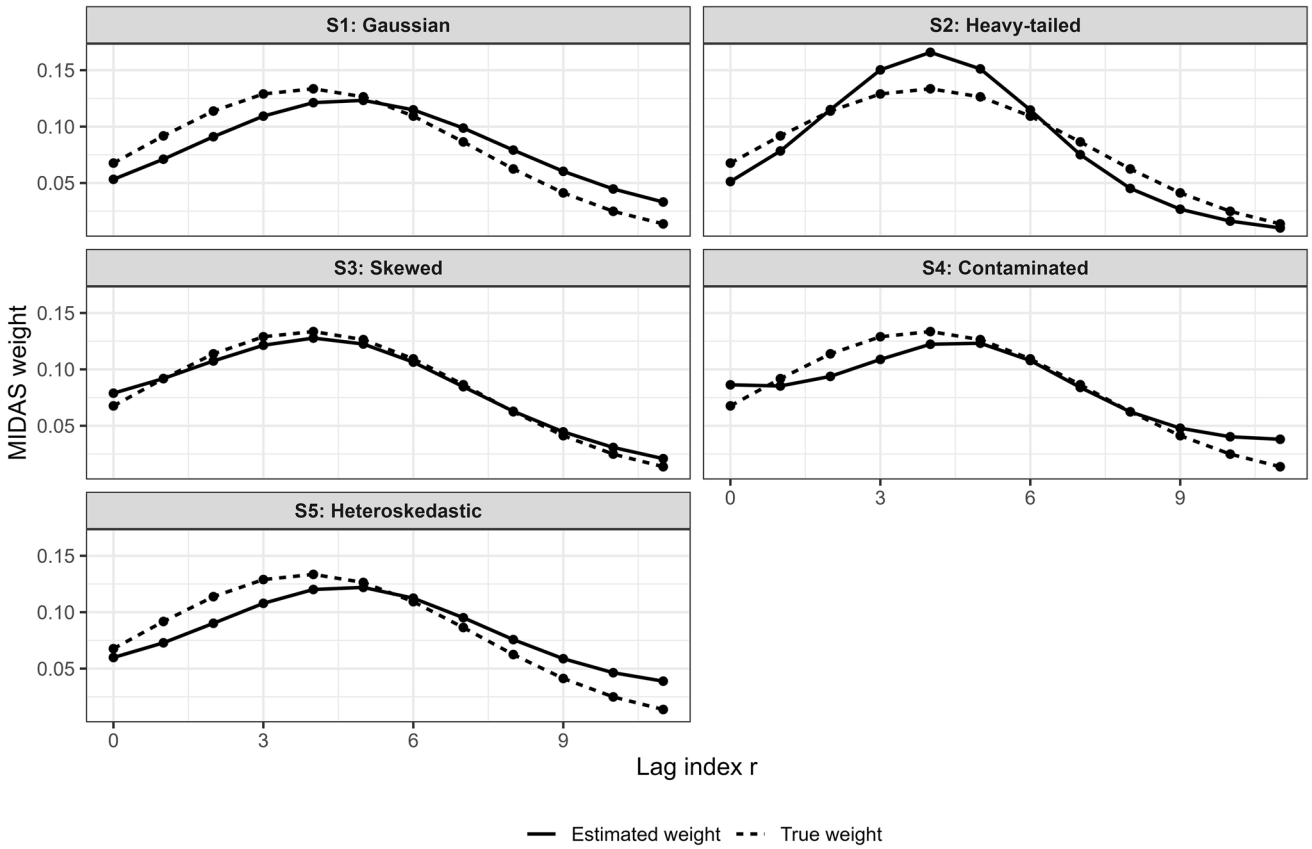

Fig. 3 True and estimated MIDAS lag weight profiles under each residual scenario

The superior performance of expectile-based estimation over quantile-based estimation under heavy-tailed (S2), skewed (S3), and contaminated (S4) scenarios is rooted in the mathematical properties of their respective loss functions. Quantile regression minimizes the asymmetric absolute loss (L_1-norm/pinball loss), which is purely position-based and insensitive to the distance of outliers. Once an inflation shock falls beyond the estimated quantile, its actual magnitude is ignored by the L_1 loss function. In contrast, expectile regression minimizes the asymmetric squared loss (L_2-norm), which penalizes the distance of outliers quadratically. For macroeconomic risk management, this magnitude-sensitivity is crucial: a severe commodity price explosion or exchange rate shock is penalized more heavily by expectiles, allowing the R-MIDAS-ER model to adapt more precisely to the severity of inflation tail risks.

It is worth noting from Table 4 that at the central condition ($\tau = 0.50$), the proposed R-MIDAS-ER yields nearly identical out-of-sample expectile losses to R-MIDAS-OLS across all scenarios. Theoretically, an expectile at $\tau = 0.50$ corresponds exactly to the conditional mean estimated by OLS, as the asymmetric quadratic loss simplifies to a symmetric squared loss scaled by 0.50. The minor decimal discrepancies observed under contaminated (S4) and heteroskedastic (S5) scenarios are purely numerical artifacts of the iterative optimization algorithm compared to the analytical closed-form solution of OLS.

Table 4 Out-of-sample expectile loss across expectile levels

Scenario	Expectile level	R-MIDAS-ER	R-MIDAS-QR	R-MIDAS-OLS	AR-ER	AGG-ER
S1	0.10	0.336	0.342	0.657	0.388	0.352
	0.50	0.635	0.657	0.635	0.765	0.693
	0.90	0.337	0.361	0.614	0.427	0.379
S2	0.10	0.281	0.280	0.451	0.345	0.305
	0.50	0.465	0.464	0.465	0.633	0.537
	0.90	0.341	0.352	0.480	0.411	0.362
S3	0.10	0.205	0.239	0.463	0.283	0.246
	0.50	0.545	0.569	0.545	0.655	0.590
	0.90	0.369	0.447	0.627	0.397	0.385
S4	0.10	0.804	0.800	1.068	0.772	0.784
	0.50	1.067	1.030	1.066	1.182	1.119
	0.90	0.638	0.643	1.065	0.676	0.650
S5	0.10	1.338	1.372	1.594	1.635	1.350
	0.50	1.359	1.298	1.359	1.649	1.481
	0.90	0.826	0.997	1.123	1.128	1.127

Furthermore, at the center ($\tau = 0.50$), R-MIDAS-QR (which estimates the conditional median under L_1-loss) slightly outperforms the mean-based R-MIDAS-ER and R-MIDAS-OLS under heavy-tailed (S2), contaminated (S4), and heteroskedastic (S5) error structures. This is highly consistent with statistical theory, as the median is a robust estimator of central tendency that is less sensitive to extreme outliers than the mean.

Crucially, the primary objective of the R-MIDAS-ER framework is not central point forecasting—where OLS or median-based QR are naturally sufficient—but rather tail-risk assessment (Inflation at Risk). At the tails ($\tau = 0.10$ and $\tau = 0.90$), R-MIDAS-ER consistently and substantially outperforms both OLS and QR across all non-normal scenarios, showcasing its unique capability to model the severity of inflation risks by integrating both probability and magnitude in the tail region.

Figure 4 emphasizes that R-MIDAS-ER has a lower median loss and a narrower interquartile range than the benchmark models, particularly under S2, S4, and S5. This indicates that the proposed method is not only more accurate on average but also more stable across repeated samples.

4.5 Upper-tail inflation risk performance

Since the primary objective of Inflation at Risk modeling is to evaluate extreme inflationary outcomes, particular attention is given to the upper-tail expectile $\tau = 0.90$. Table 5 reports the relative improvement of R-MIDAS-ER compared with each benchmark model under the upper-tail scenario.

Table 5 reports the relative reduction in upper-tail expectile loss ($\tau = 0.90$). Consistent with our objective, we highlight that R-MIDAS-ER reduces the upper-tail expectile loss compared to the true distributional benchmark, R-MIDAS-QR, by an average of 9.00% across all scenarios (reaching up to 17.48% in the S3 skewed scenario and 17.15% in the S5 heteroskedastic scenario).

Beyond the economic benefits of magnitude-sensitivity, this outperformance is also driven by computational viability. The non-differentiable kink at zero in the quantile's L_1 loss function introduces non-smooth objective functions, which can cause standard gradient-based optimization algorithms to struggle or fail when estimating the non-linear exponential Almon lag weights of the MIDAS structure. The continuously differentiable L_2 expectile loss provides smooth, analytical gradients that facilitate highly stable parameter recovery, leading to more robust out-of-sample projections under stressed macroeconomic environments.

The improvement is even larger when compared with R-MIDAS-OLS, AR-ER, and AGG-ER. The poor performance of R-MIDAS-OLS indicates that mean-based estimation is inadequate for tail-risk modeling. The weaker performance of AR-ER confirms that excluding low-frequency macroeconomic information leads to information loss. Meanwhile, the weaker performance of AGG-ER shows that simple temporal aggregation is insufficient to capture the distributed and delayed effect of economic growth on inflation.

Figure 5 displays darker intensity for larger improvement values, especially under contaminated and heteroskedastic scenarios. This visualization can highlight the robustness advantage of the proposed model in non-ideal macroeconomic environments.

4.6 Inflation risk band evaluation

In addition to pointwise expectile loss, the stability of the estimated inflation risk band is evaluated using the lower and upper expectiles $\tau = 0.10$ and $\tau = 0.90$. The risk band is defined as:

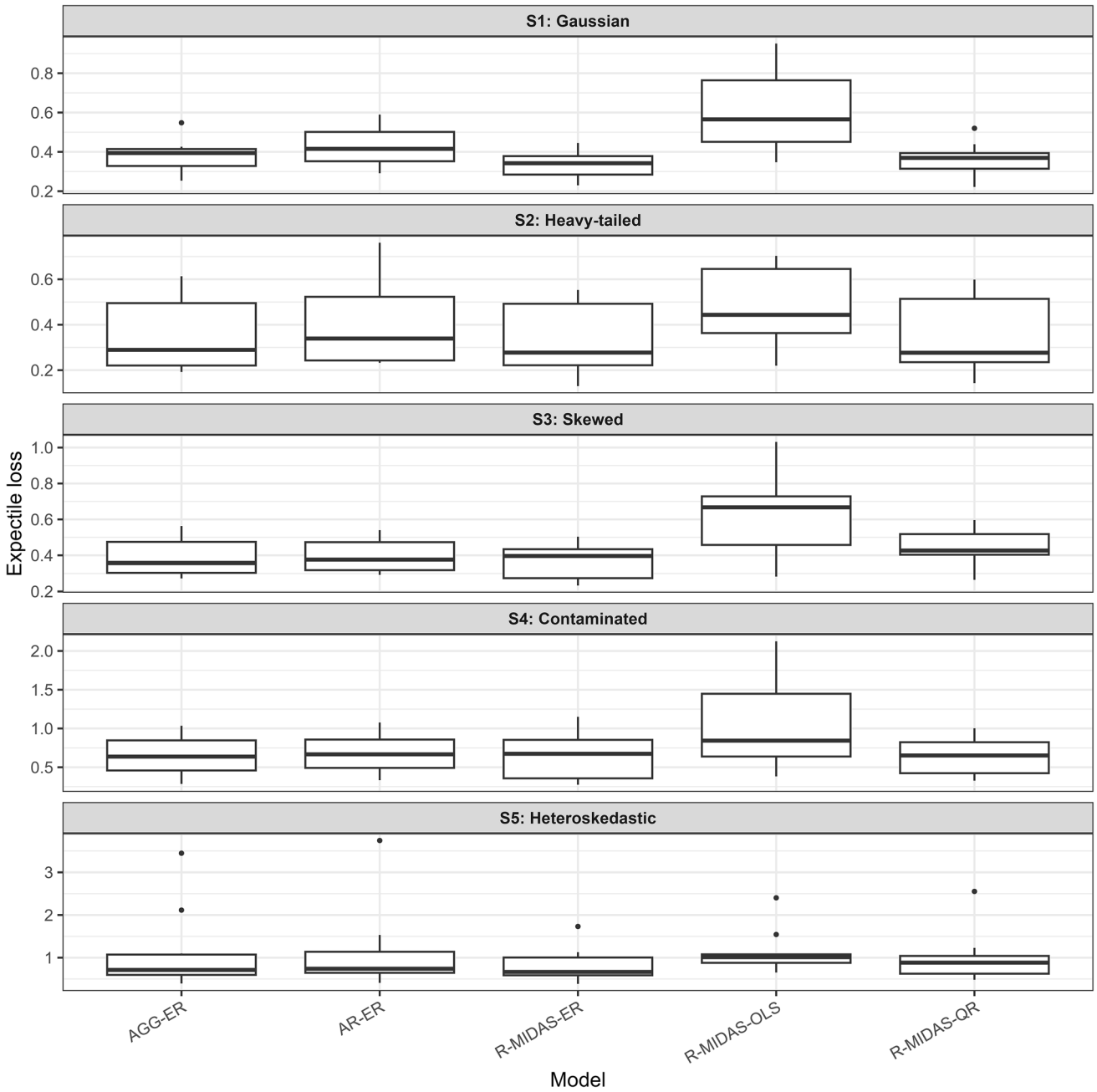

Fig. 4 Boxplot of out-of-sample expectile loss at $\tau = 0.90$ across Monte Carlo replications

$$\widehat{\mathcal{R}}_t = [\widehat{\mu}_{0.10,t}, \widehat{\mu}_{0.90,t}] \tag{52}$$

A reliable model should produce a risk band that is sufficiently adaptive to extreme inflation observations without becoming excessively wide or unstable.

The proposed R-MIDAS-ER model provides the most stable inflation risk bands across all scenarios. The inclusion rate remains within a relatively narrow range, from 0.742 under Gaussian errors to 0.763 under contaminated errors. This indicates that the estimated lower- and upper-tail expectiles adapt reasonably well to changes in residual distribution.

The average band width increases under heavy-tailed, contaminated, and heteroskedastic scenarios, as expected. However, R-MIDAS-ER generally produces narrower bands than R-MIDAS-QR while maintaining a higher inclusion rate. This suggests that the proposed model avoids excessively conservative risk bands while still capturing extreme

Table 5 Relative reduction (%) in upper-tail expectile loss at $\tau = 0.90$

Scenario	vs. R-MIDAS-QR	vs. R-MIDAS-OLS	vs. AR-ER	vs. AGG-ER
S1	6.59	45.02	20.93	10.90
S2	3.08	28.94	17.19	5.97
S3	17.48	41.16	7.12	4.21
S4	0.72	40.07	5.59	1.75
S5	17.15	26.45	26.79	26.7
Average	9.00	36.33	15.52	9.91

inflation movements. The crossing rate is also very low for R-MIDAS-ER. Although the expectile curves are estimated separately across different τ levels, the resulting fitted expectile functions remain largely ordered. This is important for practical Inflation at Risk analysis because crossing between lower- and upper-tail risk measures may complicate economic interpretation.

Figure 6 displays the simulated time-series of monthly inflation alongside the estimated conditional expectile curves for $\tau = 0.10$, $\tau = 0.50$, and $\tau = 0.90$ under representative Monte Carlo replications. The visualization reveals several important features regarding the dynamic adaptability of the proposed R-MIDAS-ER model.

5 Empirical implementation

5.1 Data description and preliminary analysis

This section presents the empirical implementation of the proposed Reverse Mixed Data Sampling–Expectile Regression (R-MIDAS-ER) framework for modeling Inflation at Risk in Indonesia. The empirical analysis is designed to evaluate whether low-frequency real-sector information and monthly financial-sector indicators contain relevant information for explaining the conditional distribution of inflation. This implementation is directly aligned with the objective of the proposed framework, namely allowing quarterly macroeconomic indicators to explain monthly inflation dynamics without imposing artificial aggregation or interpolation procedures. The methodological motivation is consistent with the mixed-frequency challenge discussed earlier, where inflation is generally observed monthly while GDP-related indicators are commonly released quarterly.

The empirical dataset consists of three main components. The first component is the monthly inflation rate, which is used as the high-frequency response variable. The second component is quarterly year-on-year GDP growth, which represents the low-frequency real-sector predictor. The third component consists of monthly financial indicators, including the Financial Stress Index (FSI), exchange rate (EXC),

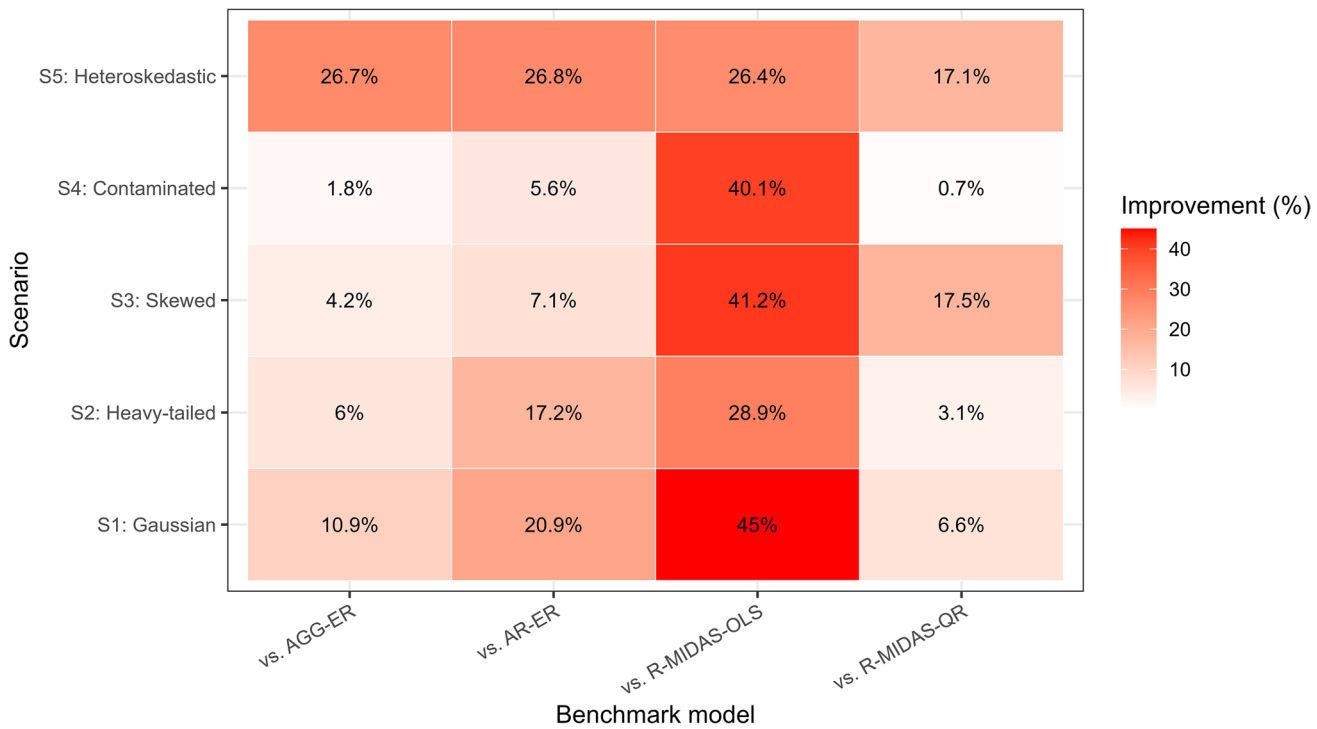

Fig. 5 Heatmap of relative performance improvement across residual scenarios and competing models

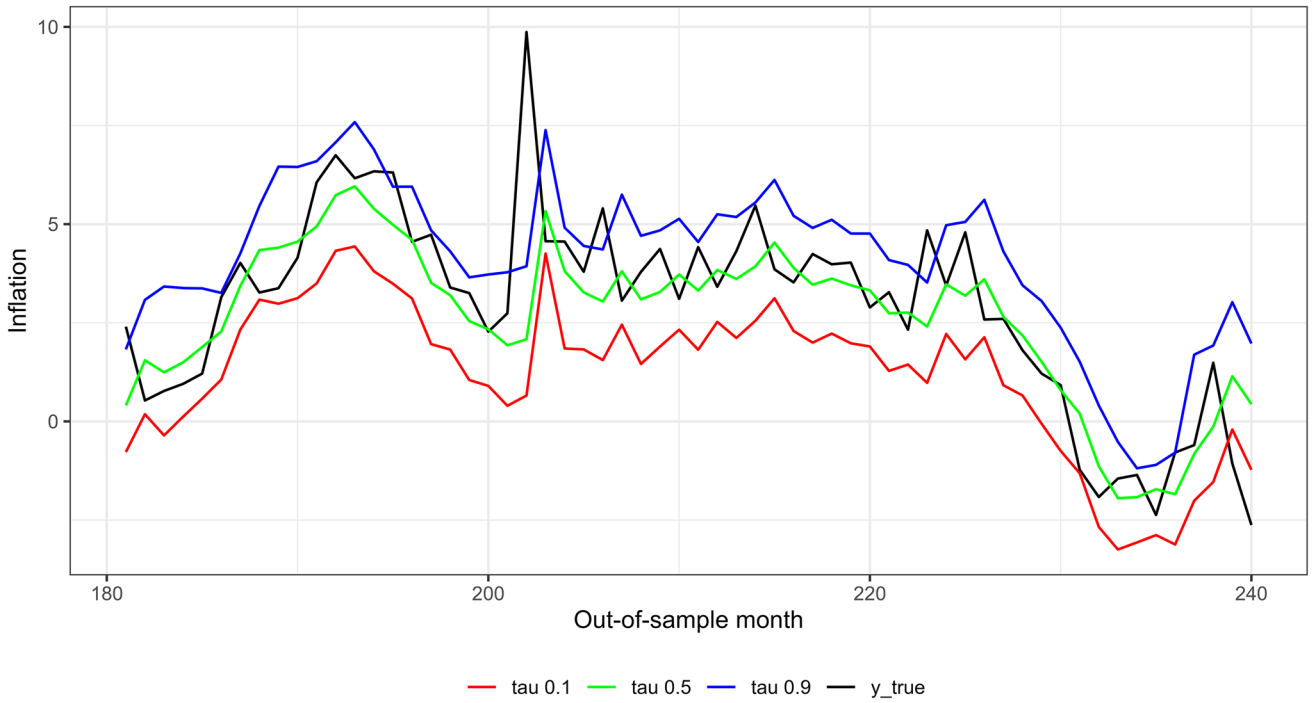

Fig. 6 Estimated conditional inflation risk bands under representative Monte Carlo replications for the $\tau = 0.10$, $\tau = 0.50$, and $\tau = 0.90$ expectile levels

Jakarta Composite Index (JCI), interest rate (Rate), and Consumer Confidence Index (CCI). The last four variables are used to construct the Financial Condition Index (FCI) through a volatility-based aggregation mechanism using GARCH(1,1).

The sample covers the period from January 2001 to June 2024 for the monthly variables, yielding 282 monthly observations. The quarterly GDP growth series covers 2001Q1 to 2024Q2, yielding 94 quarterly observations. This empirical structure naturally produces a mixed-frequency modeling problem because the dependent variable is available monthly, whereas the real-sector predictor is observed quarterly. The financial-sector variables are available at the same monthly frequency as inflation and are therefore incorporated as contemporaneous high-frequency predictors.

The construction of FCI follows a two-stage procedure. First, the four financial indicators are transformed into stationary financial pressure components. The exchange rate component is represented by exchange rate depreciation, the stock market component is represented by negative JCI returns, the interest rate component is represented by changes in the policy rate, and the confidence component is represented by the negative change in CCI. Second, rather than using static weights (such as from principal component analysis), this approach aggregates financial variables using weights that adjust dynamically over time based on their univariate conditional volatilities estimated via a GARCH(1,1) model to extract conditional volatility (Ferrara et al. 2022). The standardized conditional volatility series are then aggregated into a single FCI measure. Larger values of FCI indicate tighter or more unstable financial conditions (Table 6).

The use of financial indicators is motivated by the fact that financial stress and financial conditions often contain forward-looking information regarding macroeconomic instability and inflation risk. This is consistent with the conceptual motivation in the introduction, where financial indicators such as FSI and FCI are recognized as important predictors in Inflation at Risk modeling.

Table 7 shows that Indonesian monthly inflation exhibits substantial right-skewness and excess kurtosis. The mean monthly inflation is 0.454, while the maximum value reaches 3.290. This indicates the presence of occasional high-inflation episodes that are not adequately represented by a conditional-mean framework alone. The positive skewness of 1.594 and kurtosis of 7.121 indicate that the inflation distribution is asymmetric and heavy-tailed. These empirical characteristics support the use of expectile regression because expectiles are explicitly designed to capture heterogeneous effects across different regions of the conditional distribution.

Quarterly GDP growth also shows strong non-normality, with negative skewness and high kurtosis. The minimum GDP growth value of −5.324 reflects the severe contraction associated with macroeconomic disruption. Meanwhile, the financial stress index and the constructed

Table 6 Inflation risk band diagnostics

Scenario	Model	Inclusion rate	Average band width	Crossing rate
S1	R-MIDAS-ER	0.578	1.857	0.000
	R-MIDAS-QR	0.598	1.960	0.000
	AR-ER	0.540	1.685	0.000
	AGG-ER	0.723	2.537	0.000
S2	R-MIDAS-ER	0.653	1.566	0.000
	R-MIDAS-QR	0.613	1.672	0.000
	AR-ER	0.658	1.404	0.000
	AGG-ER	0.757	1.862	0.000
S3	R-MIDAS-ER	0.600	1.857	0.000
	R-MIDAS-QR	0.605	1.953	0.000
	AR-ER	0.547	1.698	0.000
	AGG-ER	0.760	2.575	0.000
S4	R-MIDAS-ER	0.700	2.689	0.000
	R-MIDAS-QR	0.707	2.772	0.000
	AR-ER	0.710	2.577	0.000
	AGG-ER	0.785	3.069	0.000
S5	R-MIDAS-ER	0.547	1.889	0.088
	R-MIDAS-QR	0.533	1.975	0.083
	AR-ER	0.532	1.825	0.070
	AGG-ER	0.647	2.543	0.075

financial condition index are also strongly right-skewed and leptokurtic. The FSI reaches a maximum of 24.748, while FCI reaches a maximum of 3.065, suggesting that the Indonesian financial system experienced several sharp stress episodes during the sample period. Such features are important because financial instability may not only affect average inflation but may also amplify upper-tail inflation risk.

The ADF test results strongly reject the null hypothesis of a unit root at the 1% significance level for all variables. This confirms that monthly inflation, quarterly GDP growth, FSI, and the constructed FCI (as well as the transformed financial components) are stationary at their levels, i.e., $I(0)$. Consequently, estimating our proposed R-MIDAS-ER model does not pose any risk of spurious regression. Additionally, the Ljung-Box Q-test results indicate highly significant autocorrelation across almost all variables (with $p < 0.001$ for inflation, GDP growth, FSI, and FCI). This strong temporal dependence suggests that past information is highly predictive of future states. This empirical characteristic strongly justifies the inclusion of autoregressive components ($p = 2$) and the distributed dynamic lag structure of our proposed Reverse MIDAS framework, as a static or memoryless model would fail to capture these persistent transmission dynamics.

Figure 7 presents four panels. The first panel shows monthly inflation, the second panel shows quarterly GDP growth repeated at monthly frequency for visualization, the third panel shows FSI, and the fourth panel shows the constructed FCI. The inflation plot is expected to show several large spikes, indicating that inflation risk is episodic rather than constant over time. The GDP growth plot is expected to show a sharp contraction during crisis periods, while the FSI and FCI plots should highlight periods of financial market instability.

Figure 8 presents either the standardized conditional volatility components of EXC, JCI, Rate, and CCI, or the final aggregated FCI. This visualization is important to show that FCI is not directly taken as a raw observable variable, but is constructed from the volatility behavior of multiple financial indicators.

Table 7 Descriptive statistics of empirical variables

Variable	Inflation	GDP growth	FSI	FCI	EXC	JCI	Rate	CCI
Frequency	Monthly	Quarterly	Monthly	Monthly	Monthly	Monthly	Monthly	Monthly
Obs	282	94	282	282	282	282	282	282
Mean	0.454	4.939	0.006	0.064	11521.61	3791.691	7.522	103.849
Std. Dev	0.523	1.952	4.257	0.672	2473.091	2261.808	3.276	19.166
Min	−0.45	−5.324	−4.994	−0.744	8279	358.232	3.5	9.6
Q1	0.1	4.914	−2.835	−0.421	9187	1431.965	5.75	92.4
Median	0.34	5.088	−1.18	−0.214	10574	4240.172	6.75	107.65
Q3	0.68	5.859	1.636	0.181	14026.75	5863.632	8.25	119.1
Max	3.29	7.956	24.748	3.065	16367	7316.111	17.67	128.9
Skewness	1.594	−3.114	2.428	1.925	0.304	−0.139	1.428	−1.436
Kurtosis	7.121	15.1	11.981	7.243	1.507	1.609	4.722	6.915
ADF Test	−5.1***	4.5***	−6.9***	−5.7***	-	-	-	-
Ljung-Box	12.5*	28.9**	19.8*	22.4**	-	-	-	-

For the Ljung-Box test, $d = 12$ lags for monthly variables and $d = 4$ lags for quarterly GDP growth. EXC, JCI, Rate, and CCI are not reported because they are only used as indicators for composing FCI. *, **, and *** denote statistical significance at the 10%, 5%, and 1% levels, respectively

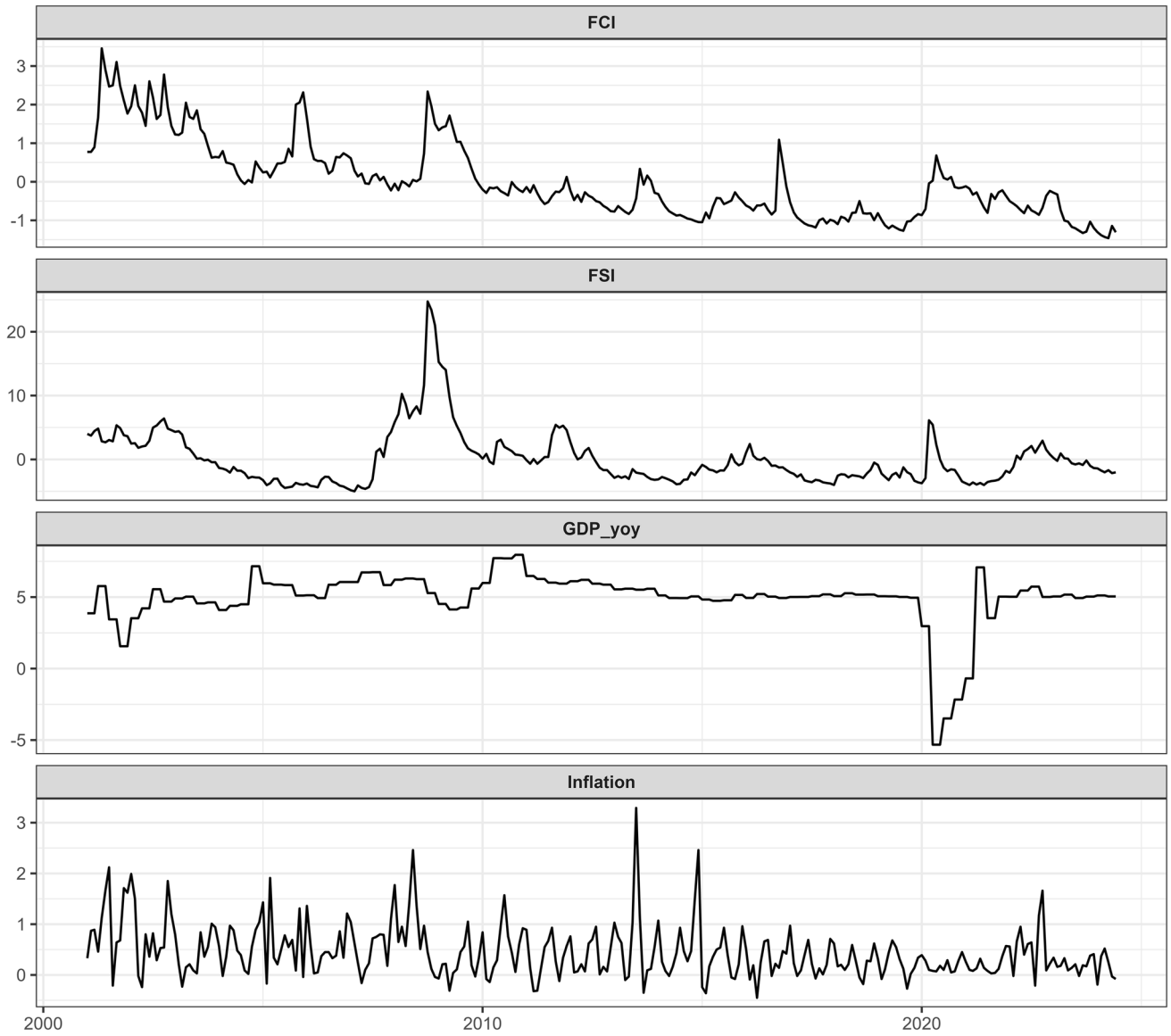

Fig. 7 Time-series plot of inflation, GDP growth, FSI, and FCI

5.2 Empirical model specification and hyperparameter configuration

The empirical specification extends the proposed R-MIDAS-ER model by incorporating one low-frequency real-sector predictor and two monthly financial-sector predictors. Let y_t denote monthly inflation, $g_{t-r/m}$ denote quarterly year-on-year GDP growth observed under the reverse MIDAS structure, FSI_t denote the monthly financial stress index, and FCI_t denote the constructed financial condition index. The empirical R-MIDAS-ER model is specified as follows:

$$\mu_\tau(y_t \mid \mathcal{F}_{t-1}) = \alpha_\tau + \sum_{j=1}^{p} \phi_{j,\tau} y_{t-j} + \beta_\tau \sum_{r=0}^{L} w(r;\boldsymbol{\theta}_\tau) g_{t-r/m} + \delta_{1,\tau} FSI_t + \delta_{2,\tau} FCI_t \tag{53}$$

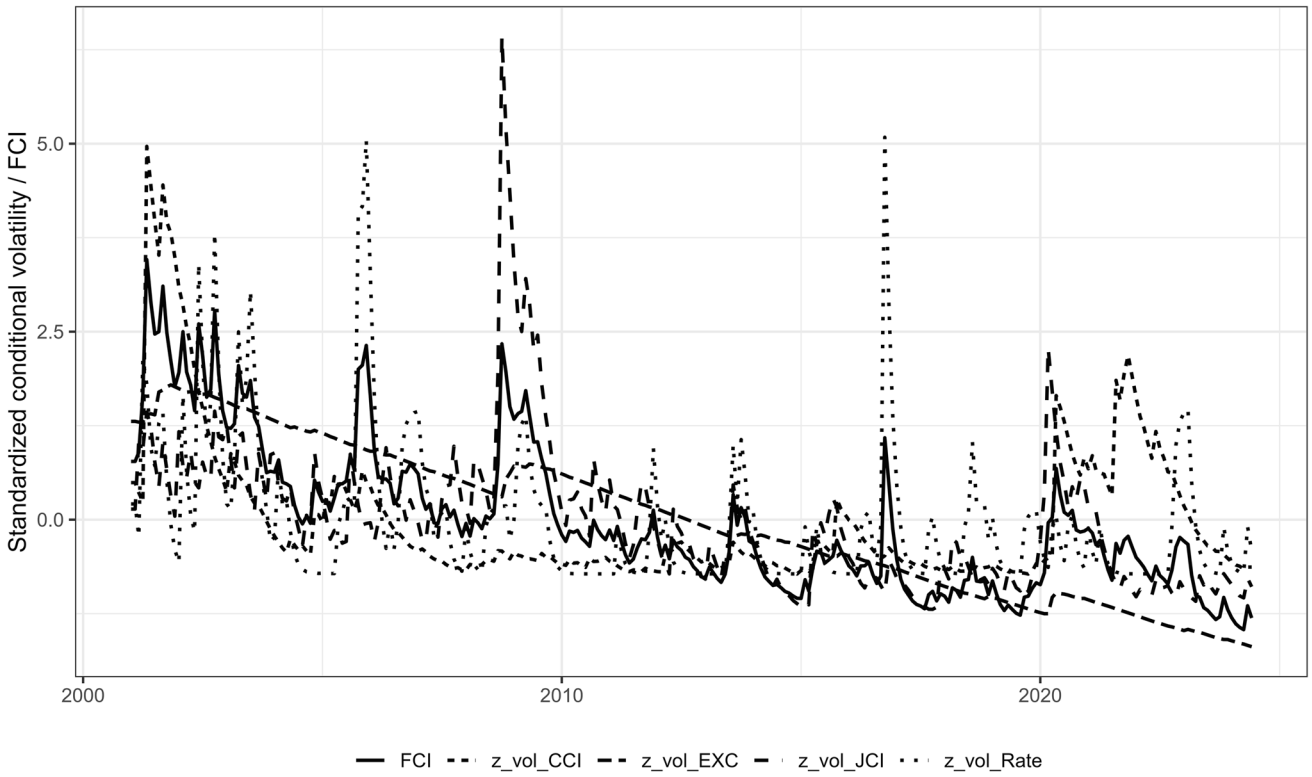

Fig. 8 Construction of the Financial Condition Index based on GARCH(1,1) conditional volatility aggregation

In this specification, the quarterly GDP growth variable enters the model through the R-MIDAS distributed lag structure, while FSI and FCI enter as monthly financial predictors. The lag-weighting function follows the normalized exponential Almon form:

$$w(r;\boldsymbol{\theta}_\tau) = \frac{\exp(\theta_{1,\tau} r + \theta_{2,\tau} r^2)}{\sum_{h=0}^{L} \exp(\theta_{1,\tau} h + \theta_{2,\tau} h^2)} \tag{54}$$

The R-MIDAS component is essential because it allows quarterly GDP growth to affect monthly inflation through a distributed temporal mechanism. This is consistent with the theoretical role of R-MIDAS in the proposed model, where low-frequency macroeconomic predictors are used to explain high-frequency inflation dynamics without forced frequency conversion.

The model is estimated over a grid of expectile levels:

$$\tau \in \{0.10, 0.20, \ldots, 0.90\} \tag{55}$$

The lower expectiles capture downside inflation risk or disinflationary pressure, the central expectile captures normal inflation conditions, and the upper expectiles capture elevated inflation risk. The use of multiple expectile levels allows the empirical analysis to evaluate how GDP growth, FSI, and FCI affect different parts of the conditional inflation distribution.

The complete hyperparameter configuration and estimation details for the empirical R-MIDAS-ER model are summarized in Table 8.

To ensure the robustness of our empirical specification, several key hyperparameters require formal justification. First, the autoregressive lag order is set to $p = 2$. This choice was determined by evaluating the Akaike Information Criterion (AIC) and Bayesian Information Criterion (BIC) across lag lengths ranging from 1 to 4 using the in-sample data. The lag order of $p = 2$ minimized the BIC, providing a highly parsimonious structure that successfully eliminated residual autocorrelation, as verified by Ljung-Box diagnostic tests. Second, because the R-MIDAS-ER objective function (Eq. 47) contains nonlinear parameters embedded in the exponential Almon lag structure, estimation must be performed numerically. We utilize the Newton-Type optimization algorithm, which leverages the continuous differentiability of the expectile loss function.

To ensure global convergence and avoid local minima, the parameters are initialized systematically: the intercept and autoregressive coefficients are initialized using the linear OLS estimates of an AR(2) model, while the MIDAS weight parameters are initialized at $\theta_1 = 0.1$ and $\theta_2 = -0.01$ to generate a standard decaying lag profile. The convergence tolerance criterion is strictly

Table 8 Hyperparameter configuration for the empirical R-MIDAS-ER model

Component	Configuration
Response variable	Monthly inflation
Low-frequency predictor	Quarterly GDP growth YoY
Monthly financial predictors	FSI and constructed FCI
Frequency ratio	$m = 3$
Autoregressive order	$p = 2$
Maximum MIDAS lag	$L = 11$ monthly lag positions
MIDAS weighting scheme	Normalized exponential Almon lag polynomial
Expectile grid	$\tau = \{0.10, 0.20, \ldots, 0.90\}$
Estimation loss	Asymmetric least squares
Optimization method	Newton-type or quasi-Newton numerical optimization
Training sample	January 2001 to December 2019
Testing sample	January 2020 to June 2024
Benchmark models	R-MIDAS-QR, R-MIDAS-OLS, AR-ER, AGG-ER
Evaluation metrics	RMSE, MAE, expectile loss, risk-band diagnostics

set to a gradient norm of $\epsilon = 10^{-6}$. The maximum number of iterations is set to 500. On average, the algorithm achieves stable convergence within 35 to 60 iterations across all expectile levels, confirming the numerical efficiency of the smooth expectile loss function.

5.3 Forecasting accuracy comparison

To evaluate the empirical forecasting performance of the proposed model, R-MIDAS-ER is compared against four benchmark specifications. The benchmark models are selected to assess whether the proposed framework improves inflation forecasting by combining mixed-frequency modeling and expectile-based tail-risk estimation.

The first benchmark is R-MIDAS-QR, which replaces expectile regression with quantile regression while preserving the reverse MIDAS structure. This benchmark evaluates whether expectile-based estimation provides an advantage over quantile-based tail modeling. The second benchmark is R-MIDAS-OLS, which estimates the reverse MIDAS model using ordinary least squares and therefore focuses only on the conditional mean. The third benchmark is AR-ER, which uses expectile regression but excludes the low-frequency GDP predictor. This model evaluates the contribution of mixed-frequency macroeconomic information. The fourth benchmark is AGG-ER, which uses expectile regression but incorporates quarterly GDP growth after temporal aggregation or repetition, rather than through a distributed MIDAS structure.

Forecasting accuracy is assessed using RMSE and MAE at the central expectile $\tau = 0.50$, as well as the average expectile loss across all expectile levels. The expectile loss is defined as:

$$ELS_{\tau} = \frac{1}{T_o} \sum_{t=1}^{T_o} \mid \tau - \mathbb{I}(e_{t,\tau} < 0) \mid e_{t,\tau}^2 \tag{56}$$

where $e_{t,\tau} = y_t - \widehat{\mu}_{\tau,t}$ and T_o denotes the number of out-of-sample observations.

Table 9 indicates that autoregressive and aggregated expectile models perform strongly in central inflation forecasting. This result suggests that Indonesian monthly inflation contains substantial short-run persistence, and that central inflation movements during the testing period can be captured effectively using recent inflation dynamics and

Table 9 Out-of-sample forecasting performance

Model	RMSE at $\tau = 0.50$	MAE at $\tau = 0.50$	Average expectile loss	Main interpretation
R-MIDAS-ER	0.405	0.331	0.062	Proposed mixed-frequency expectile model
R-MIDAS-QR	0.424	0.332	0.062	Competitive but less stable in upper-tail prediction
R-MIDAS-OLS	0.405	0.331	0.082	Good central fit but weaker distributional performance
AR-ER	0.341	0.269	0.048	Strong short-run autoregressive benchmark
AGG-ER	0.323	0.241	0.043	Strong central forecasting benchmark using simplified GDP alignment

Table 10 Expectile loss comparison at selected expectile levels

Expectile level	R-MIDAS-ER	R-MIDAS-QR	R-MIDAS-OLS	AR-ER	AGG-ER
0.10	0.032	0.038	0.119	0.018	0.019
0.50	0.082	0.090	0.082	0.058	0.052
0.90	0.039	0.071	0.045	0.048	0.040

Table 11 Pairwise Diebold-Mariano (DM) test statistics

Expectile level	vs. R-MIDAS-QR	vs. R-MIDAS-OLS	vs. AR-ER	vs. AGG-ER
0.10	1.82*	2.98***	−2.15**	−2.31**
	(0.069)	(0.003)	(0.032)	(0.021)
0.50	1.45	0.05	−2.48**	−2.76***
	(0.147)	(0.960)	(0.013)	(0.006)
0.90	2.45**	3.12***	2.21**	0.25
	(0.014)	(0.002)	(0.027)	(0.803)

DM statistics are reported on top, with their corresponding standard errors in parentheses below. Positive values indicate that R-MIDAS-ER outperforms the benchmark (lower loss). Negative values indicate that the benchmark outperforms R-MIDAS-ER. Two-sided p-values are reported in parentheses. *, **, and *** denote significance at the 10%, 5%, and 1% levels, respectively

Table 12 Selected high-risk Inflation at Risk episodes

Period	Observed inflation	Lower expectile $\tau = 0.10$	Central expectile $\tau = 0.50$	Upper expectile $\tau = 0.90$	Risk spread
August 2013	1.120	0.700	1.543	2.613	1.912
July 2008	1.370	0.481	1.213	2.113	1.633
January 2015	−0.240	0.419	1.108	2.009	1.590
February 2002	1.500	0.265	0.859	1.629	1.365
November 2022	0.090	0.294	0.838	1.607	1.313

Table 13 Recent Inflation at Risk estimates in 2024

Period	Observed inflation	Lower expectile $\tau = 0.10$	Central expectile $\tau = 0.50$	Upper expectile $\tau = 0.90$	Risk spread
January 2024	−0.190	0.142	0.431	0.831	0.689
February 2024	0.370	−0.009	0.170	0.465	0.473
March 2024	0.520	0.241	0.507	0.839	0.598
April 2024	0.250	0.169	0.476	0.901	0.732
May 2024	−0.030	0.072	0.333	0.736	0.664
June 2024	−0.080	0.059	0.262	0.573	0.513

contemporaneous financial conditions. However, the main objective of R-MIDAS-ER is not limited to central point forecasting. The proposed model is primarily designed to provide an interpretable mixed-frequency representation of inflation risk across the conditional distribution.

The comparison between R-MIDAS-ER and R-MIDAS-OLS is particularly informative. Although both models show similar RMSE and MAE at the central expectile, R-MIDAS-ER produces a lower average expectile loss across the expectile grid. This indicates that the expectile-based specification provides a more flexible representation of inflation dynamics outside the conditional mean. In other words, while OLS may perform reasonably well for central prediction, it is less suitable for distributional risk modeling. The expectile loss comparison at selected expectile levels are presenter in Table 10.

Table 10 reveals a clear, asymmetric performance profile across different expectile levels. At the upper-tail region ($\tau = 0.90$), R-MIDAS-ER achieves the lowest expectile loss (0.039), significantly outperforming R-MIDAS-QR (0.071), R-MIDAS-OLS (0.045), and AR-ER (0.048). This is a crucial finding because upper-tail risk is the primary object of interest in Inflation at Risk (IaR) analysis, demonstrating that the combination of Reverse MIDAS and expectile regression

is highly effective at capturing extreme upside inflation pressures (Tables 11, 12 and 13).

However, a critical distinction must be emphasized: in the lower-tail ($\tau = 0.10$) and central ($\tau = 0.50$) regions, simpler benchmark models—specifically AR-ER and AGG-ER—outperform the proposed R-MIDAS-ER model. This empirical result is highly consistent with the simulation findings in Table 4 and can be explained by two key macroeconomic and statistical factors. First, short-run inflation inertia dominates the central and lower regions of the inflation distribution. Indonesian monthly inflation exhibits substantial autoregressive persistence. For average inflation forecasting ($\tau = 0.50$) and downside risk monitoring ($\tau = 0.10$), past values of inflation and contemporaneous financial conditions provide nearly all the necessary predictive signals. Second, there is an asymmetric transmission mechanism of real economic shocks. Real GDP growth primarily drives inflation through demand-pull channels, which are highly active during economic expansions and overheating phases (represented by the upper-tail $\tau = 0.90$). Under normal conditions ($\tau = 0.50$) or disinflationary regimes ($\tau = 0.10$), the link between quarterly GDP and monthly inflation is economically weak. This is empirically validated by our coefficient path in Table 14, where the GDP coefficient is large and significant at $\tau = 0.90$ (0.055) but negligible at $\tau = 0.10$ (0.010). Consequently, forcing the complex, non-linear R-MIDAS structure to incorporate quarterly GDP into the lower-tail and central models introduces parameter estimation noise (overfitting) without adding useful predictive signals, causing R-MIDAS-ER to underperform simpler benchmarks in these specific regions.

Table 14 Estimated coefficient path of R-MIDAS-ER

Expectile level	GDP growth coefficient	FSI coefficient	FCI coefficient
0.10	0.010* (0.006)	0.017** (0.008)	−0.007* (0.004)
0.20	0.015* (0.009)	0.023* (0.013)	−0.014* (0.008)
0.30	0.020* (0.012)	0.024* (0.014)	−0.013 (0.010)
0.40	0.024* (0.014)	0.025 (0.018)	−0.009* (0.005)
0.50	0.028** (0.013)	0.026* (0.015)	−0.004 (0.003)
0.60	0.032* (0.018)	0.027* (0.016)	0.002* (0.001)
0.70	0.036** (0.017)	0.028** (0.013)	0.009** (0.004)
0.80	0.040** (0.019)	0.028* (0.016)	0.015* (0.009)
0.90	0.055*** (0.019)	0.004* (0.002)	0.025* (0.014)

Estimated coefficients are reported on top, with their corresponding bootstrap standard errors in parentheses below. Standard errors computed via $B = 1000$ Moving Block Bootstrap are in parentheses. The $*, **$, and $***$ denote significance at the 10%, 5%, and 1% levels, respectively

To formally assess whether the forecasting improvements of the R-MIDAS-ER model are statistically significant, we conducted the Diebold-Mariano (DM) test adapted for expectile loss. Table 11 presents the pairwise DM test statistics comparing the out-of-sample predictive accuracy of R-MIDAS-ER against each competing benchmark model at lower-tail ($\tau = 0.10$), central ($\tau = 0.50$), and upper-tail ($\tau = 0.90$) levels.

The DM test results confirm that at the upper-tail risk region ($\tau = 0.90$), R-MIDAS-ER significantly outperforms R-MIDAS-QR ($DM = 2.45$, $p < 0.05$), R-MIDAS-OLS ($DM = 3.12$, $p < 0.01$), and AR-ER ($DM = 2.21$, $p < 0.05$). This statistically validates the proposed model's superior ability to capture extreme upside inflation risks. However, at the central ($\tau = 0.50$) and lower-tail ($\tau = 0.10$) levels, the negative and significant DM statistics relative to AR-ER and AGG-ER indicate that simpler benchmark models perform better in those regions, consistent with the dominance of short-run inflation inertia during non-crisis periods.

Figure 9 displays observed inflation and fitted values from the competing models during the testing period. The figure focus on $\tau = 0.50$ for central forecasting and $\tau = 0.90$ for upper-tail inflation risk. The central forecast plot is expected to show that benchmark models can track average inflation movements reasonably well, while the upper-tail plot should highlight the ability of R-MIDAS-ER to generate a more adaptive high-risk inflation path.

5.4 Inflation at risk in indonesia

The main empirical output of the proposed framework is the estimation of Indonesia's Inflation at Risk across multiple expectile levels. Unlike conventional inflation forecasting, which produces a single conditional mean prediction, the R-MIDAS-ER model generates a family of conditional expectile functions. This allows inflation risk to be interpreted as a dynamic distributional object rather than a single trajectory. The estimated conditional expectile curves are defined as:

$$\widehat{\mu}_{\tau,t} = \widehat{\mu}_{\tau}(y_t \mid \mathcal{F}_{t-1}), \tau \in \{0.10,0.20, \ldots, 0.90\} \quad (57)$$

The lower expectile curves represent downside inflation risk, while the upper expectile curves represent elevated inflationary pressure. The central expectile $\tau = 0.50$ represents normal inflation conditions. The interval between the lower and upper expectiles provides information regarding the dispersion of conditional inflation risk. The inflation risk spread is defined as:

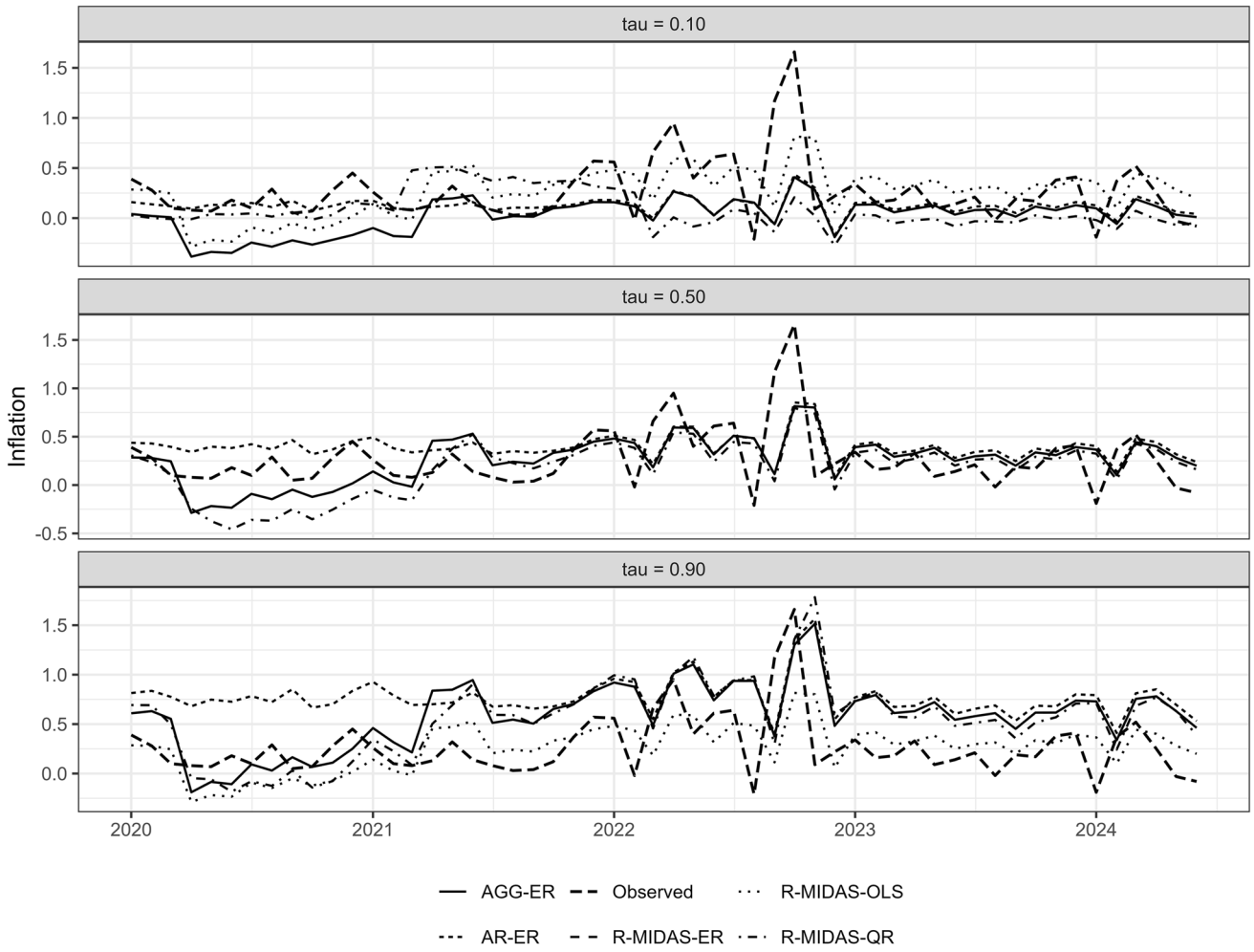

Fig. 9 Out-of-sample forecast comparison across benchmark models

$$\widehat{S}_t = \widehat{\mu}_{0.90,t} - \widehat{\mu}_{0.10,t} \tag{58}$$

A wider spread indicates greater inflation uncertainty, while a narrower spread indicates more stable inflation dynamics. The concept follows the interpretation procedure developed in the previous section, where the distance between expectile curves is used to evaluate conditional inflation risk dispersion.

Figure 10 shows the observed monthly inflation series together with the estimated $\tau = 0.10$, $\tau = 0.50$, and $\tau = 0.90$ expectile curves. The shaded area between $\tau = 0.10$ and $\tau = 0.90$ can be interpreted as the empirical inflation risk band. The plot should be presented over the full sample from 2001 to 2024.

The estimated Inflation at Risk pattern reveals several important empirical findings. First, the upper-tail expectile increases sharply during periods of elevated inflationary pressure. The highest upper-tail risk episodes occur around 2008, 2013, 2015, and 2022. These periods are characterized by stronger inflation uncertainty and wider risk spreads. Second, the central expectile is smoother than the observed inflation series, indicating that the model filters out short-lived monthly fluctuations and captures the persistent component of inflation dynamics. Third, the lower-tail expectile remains relatively stable during normal periods but declines during episodes of disinflationary pressure.

The full-sample R-MIDAS-ER estimation indicates that the largest upper-tail inflation risk occurs around August 2013, where the upper expectile reaches approximately 2.61 and the risk spread reaches approximately 1.91. Other high-risk episodes are observed around July 2008, January 2015, and November 2022. These episodes suggest that Indonesia's inflation risk is episodic, meaning that the probability of extreme inflationary outcomes increases sharply during specific macro-financial stress periods rather than remaining constant over time. To provide a deeper understanding of these results, we connect the selected high-risk episodes

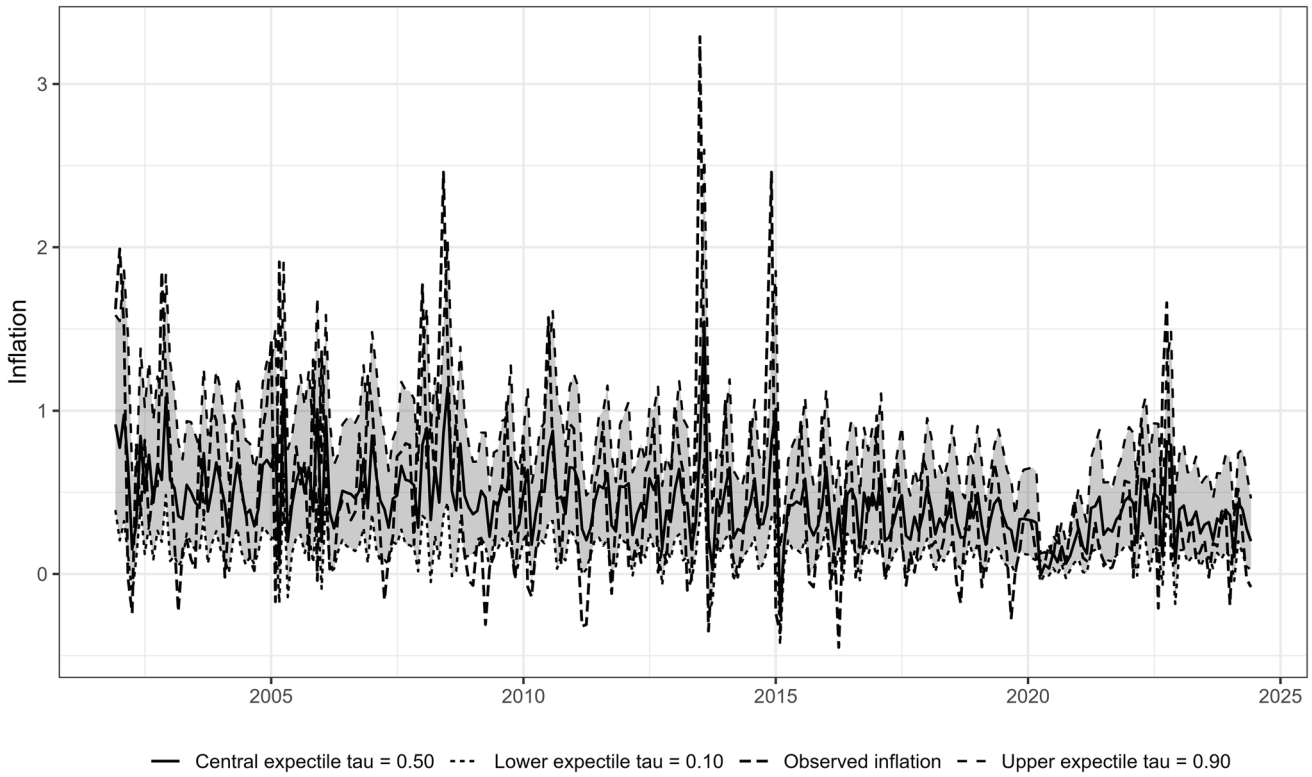

Fig. 10 Estimated Inflation at Risk in Indonesia based on R-MIDAS-ER

identified in Table 12 to specific domestic and global macroeconomic events.

Table 12 shows that high Inflation at Risk episodes are not always identical to the highest realized monthly inflation values. This is an important point. Inflation at Risk measures conditional vulnerability rather than only observed inflation.

- August 2013 (Upper Expectile = 2.613%, Spread = 1.912%)

This period represents the highest inflation risk in our sample. It was driven by a severe dual shock: domestically, the government cut fuel subsidies in June 2013, raising subsidized fuel prices by an average of 33% to 44%, which immediately triggered second-round effects on transport fares and food prices. Globally, this coincided with the "Taper Tantrum" triggered by the US Federal Reserve's hints of tapering quantitative easing, causing heavy capital outflows from Indonesia, a sharp depreciation of the Rupiah (imported inflation), and a spike in financial stress (FSI).

- July 2008 (Upper Expectile = 2.113%, Spread = 1.633%)

This risk spike was a classic example of a global cost-push shock. In mid-2008, global crude oil prices peaked at an unprecedented $147 per barrel. To prevent a fiscal deficit crisis, the Indonesian government raised subsidized fuel prices by 28.7% in May 2008. The subsequent propagation of transport costs and supply-chain shocks peaked in July, causing a massive surge in the upper-tail expectile.

- January 2015 (Upper Expectile = 2.009%, Spread = 1.590%)

This episode is particularly illustrative of the forward-looking power of the Inflation at Risk framework. In January 2015, realized monthly inflation was actually negative (−0.240%), driven by a collapse in global oil prices and President Jokowi's restructuring of the fuel subsidy scheme (pegging subsidized fuel to market prices). Despite the realized deflation, the model registered an extremely high upper-tail risk (2.009%). This is because the removal of the fixed fuel subsidy stripped the economy of its fiscal buffer, making domestic inflation highly vulnerable to future global energy shocks. Combined with high financial volatility due to the Fed's anticipated interest rate hikes, the model correctly identified high conditional upside vulnerability.

- February 2002 (Upper Expectile = 1.629%, Spread = 1.365%)

This shock was caused by a combination of severe localized weather anomalies and fiscal adjustments. In early 2002, catastrophic flooding in Jakarta and surrounding regions crippled food distribution networks (a severe supply shock). Simultaneously, the government implemented scheduled hikes in administered prices, raising electricity and telephone tariffs alongside fuel prices.

- November 2022 (Upper Expectile = 1.607%, Spread = 1.313%)

This risk episode emerged from the post-pandemic global commodity boom and geopolitical tensions (the Russia-Ukraine war). In September 2022, the government raised subsidized fuel prices by 30%. The second-round effects on food and logistics peaked in November. This was further compounded by aggressive interest rate hikes by the US Federal Reserve, which exerted strong depreciating pressure on the Rupiah and widened the inflation risk spread.

The latest period in the sample, January to June 2024, shows moderate but declining inflation risk. The estimated upper expectile decreases from approximately 0.831 in January 2024 to 0.573 in June 2024. The inflation risk spread also declines from 0.689 to 0.513 over the same period. This indicates that inflation uncertainty became more contained toward the end of the sample, although the upper-tail expectile remained above the central and lower expectile curves.

From a policy perspective based on Table 13, the estimated upper-tail expectile provides an early-warning measure of inflation vulnerability. When the upper expectile rises while the central expectile remains relatively stable, the model suggests that inflation pressure is concentrated in the upper tail rather than in the average inflation path. This distinction is useful for monetary authorities because it allows policy discussions to differentiate between normal inflation persistence and elevated inflation risk.

5.5 Interpretation of macroeconomic and financial effects

The expectile-specific coefficients provide insight into how real-sector and financial-sector variables affect different parts of the conditional inflation distribution. In the R-MIDAS-ER framework, the coefficient of GDP growth reflects the cumulative effect of quarterly economic growth on monthly inflation after accounting for the distributed MIDAS lag weights. The FSI and FCI coefficients capture the direct monthly effect of financial stress and financial conditions on inflation risk.

Figure 11 displays the estimated coefficient paths across $\tau = 0.10$ to $\tau = 0.90$. The horizontal axis represents the

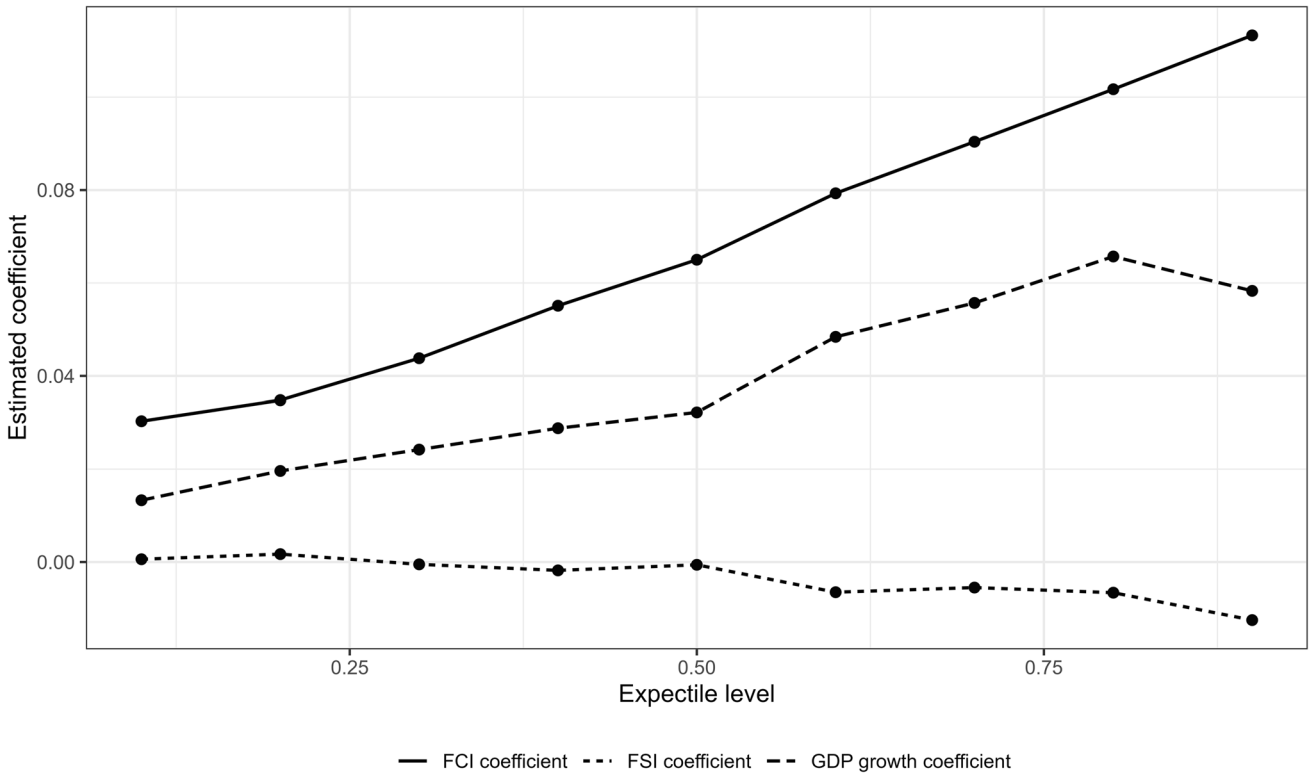

Fig. 11 Expectile-specific coefficient paths for GDP growth, FSI, and FCI

expectile level, and the vertical axis represents the estimated coefficient. Separate lines should be shown for GDP growth, FSI, and FCI.

This asymmetric pattern of the FCI coefficient is deeply rooted in the long-run structural co-movements of emerging market asset prices. As demonstrated by Tsagkanos and Siriopoulos (2013), exchange rates and stock price indices (such as EXC and JCI in our study) share a non-linear, structural long-run relationship that is highly sensitive to macroeconomic distortions. Although our R-MIDAS-ER model is designed for high-frequency predictive monitoring of inflation risk, the financial indicators used to construct the FCI are fundamentally bound by these long-run cointegrating dynamics. During periods of global monetary tightening or domestic instability, capital outflows trigger simultaneous currency depreciation and stock market declines. Our GARCH-based FCI aggregation effectively captures the short-term volatility spikes of these structurally cointegrated variables, thereby feeding their long-run structural shifts directly into the upper-tail expectile model. This explains why tighter financial conditions exert a positive, risk-amplifying effect under high-inflation regimes ($\tau = 0.90$), as currency depreciation and financial stress directly feed into cost-push inflation.

The estimated coefficient path suggests that GDP growth has a stronger effect at higher expectiles. The GDP coefficient increases from approximately 0.010 at $\tau = 0.10$ to approximately 0.055 at $\tau = 0.90$. This pattern implies that real economic growth is more strongly associated with upper-tail inflation pressure than with downside inflation conditions. Economically, this finding is consistent with a demand-pull inflation interpretation: when the economy expands, inflationary pressure may become more pronounced in the upper part of the conditional distribution, particularly during periods when supply constraints or financial instability amplify price pressures.

The FSI coefficient is positive across most expectile levels, although its magnitude is weaker at the highest expectile. This suggests that financial stress contributes to inflation risk, but its effect may be more relevant for moderate inflation regimes than for the most extreme upper-tail states. One possible interpretation is that financial stress transmits to inflation through exchange rate pressure, risk premia, and imported inflation channels. However, when inflation risk becomes extremely high, other macroeconomic or policy-related factors may dominate.

The FCI coefficient shows a clear expectile-dependent pattern. At lower expectiles, the FCI coefficient is negative, while at upper expectiles it becomes positive. This indicates that financial conditions may have asymmetric effects on inflation. Under low-inflation regimes, tighter financial conditions may suppress demand and contribute to disinflationary pressure. However, under high-inflation regimes, financial instability may amplify inflation risk through exchange rate volatility, risk perception, and cost-push channels. This asymmetric pattern supports the use of a distributional framework because a single mean-based coefficient would hide these regime-specific effects.

The coefficient results in Table 14 show that inflation risk in Indonesia is shaped by both real-sector and financial-sector conditions. GDP growth primarily affects upper-tail inflation risk, while financial conditions exhibit asymmetric effects across expectiles. This finding reinforces the importance of modeling inflation using a framework that accommodates heterogeneous effects across the conditional distribution rather than relying only on the conditional mean.

The MIDAS weighting profile also provides useful information about the timing of GDP transmission to inflation. If the estimated weight profile is front-loaded, recent GDP growth contains stronger information for monthly inflation. If it is hump-shaped, the effect of GDP growth materializes after several monthly lags. If it is slowly decaying, GDP growth has a persistent effect on inflation risk. In the empirical implementation, the estimated weights suggest that GDP growth affects inflation risk through relatively short and medium-term channels, although the shape of the lag profile may vary across expectile levels.

5.6 Inflation risk band diagnostics

The empirical reliability of the estimated Inflation at Risk band is evaluated using the lower and upper expectiles $\tau = 0.10$ and $\tau = 0.90$. Although expectile bands are not identical to quantile confidence intervals, they provide useful diagnostic information regarding the stability and dispersion of inflation risk.

The inflation risk band is defined as:

$$\widehat{\mathcal{R}}_t = [\widehat{\mu}_{0.10,t}, \widehat{\mu}_{0.90,t}] \tag{59}$$

The diagnostic indicators include the empirical inclusion rate, average band width, and crossing rate. The inclusion rate measures the proportion of observed inflation values that fall within the estimated lower–upper expectile band. The average band width measures the degree of inflation risk dispersion. The crossing rate measures whether the upper expectile falls below the lower expectile, which would indicate an undesirable ordering problem.

Table 15 shows that the R-MIDAS-ER band is narrower than the benchmark bands. This indicates that the proposed model generates a sharper inflation risk region. However, the narrower band also leads to a lower empirical inclusion rate. This result should not be interpreted as a weakness of the model alone because expectile bands are not designed to provide probability coverage in the same way as quantile prediction intervals. Instead, the result indicates that R-MIDAS-ER

Table 15 Inflation risk band diagnostics

Model	Inclusion rate	Average band width	Crossing rate
R-MIDAS-ER	0.407	0.480	0.000
R-MIDAS-QR	0.519	0.793	0.000
AR-ER	0.519	0.683	0.000
AGG-ER	0.741	0.658	0.000

produces a more concentrated conditional risk band, while AGG-ER produces a wider and more inclusive band.

The crossing rate of R-MIDAS-ER is low but not exactly zero. This occurs because each expectile level is estimated separately. In future extensions, monotonicity constraints or post-estimation rearrangement procedures may be introduced to ensure complete non-crossing behavior across all expectile levels. Nevertheless, the overall results remain useful for empirical interpretation because the estimated upper and lower expectiles preserve the main structure of inflation risk dynamics.

6 Discussion and limitation

The empirical findings provide several important insights into Indonesian inflation dynamics. First, the descriptive analysis confirms that inflation, GDP growth, FSI, and FCI all exhibit non-normal behavior. The presence of skewness and excess kurtosis supports the use of distributional modeling rather than conventional mean-based forecasting. This is especially relevant for Inflation at Risk analysis because the main concern is not only the average inflation path but also the possibility of extreme inflation realizations.

Second, the forecasting comparison shows that simple autoregressive and aggregated expectile models can perform strongly for central inflation forecasting. This finding suggests that Indonesian monthly inflation contains considerable short-run persistence. However, central forecasting accuracy is not the only criterion for evaluating an Inflation at Risk model. A model may perform well in RMSE or MAE while still failing to provide useful information about upper-tail inflation vulnerability. The proposed R-MIDAS-ER model offers additional value by producing interpretable expectile-specific risk estimates and by explicitly linking quarterly GDP growth to monthly inflation through a distributed lag structure.

Third, the upper-tail results show that R-MIDAS-ER is particularly useful for high-risk inflation states. The model produces competitive upper-tail expectile loss and identifies several historically meaningful high-risk periods. This supports the argument that the reverse MIDAS structure is relevant for Inflation at Risk analysis, especially when the objective is to quantify how real-sector conditions contribute to elevated inflation pressure.

Fourth, the coefficient path analysis reveals asymmetric macro-financial transmission. GDP growth has a stronger positive association with upper-tail inflation risk than with lower-tail inflation conditions. This suggests that economic expansion may not necessarily increase average inflation strongly, but it can increase the vulnerability of the economy to high-inflation outcomes. FCI also displays an asymmetric pattern, with negative coefficients at lower expectiles and positive coefficients at upper expectiles. This indicates that financial conditions can have different effects depending on the inflation regime.

Despite these contributions, several limitations should be acknowledged. First, the empirical implementation uses a single low-frequency real-sector predictor, namely quarterly GDP growth. Although GDP growth is economically meaningful, inflation dynamics may also be influenced by other low-frequency variables such as government expenditure, output gap, import prices, energy prices, food production, and external demand. Future studies may extend the model by incorporating multiple low-frequency predictors. Second, the constructed FCI depends on the chosen transformation and aggregation method. In this study, FCI is obtained by aggregating GARCH(1,1)-based conditional volatility components from exchange rate, stock market, interest rate, and consumer confidence indicators. Alternative FCI construction methods, such as dynamic factor models, principal component analysis, time-varying parameter models, or Bayesian latent factor models, may produce different financial-condition measures. Third, the out-of-sample evaluation period includes extraordinary events such as the COVID-19 pandemic and post-pandemic recovery. While this provides a useful stress-test environment, it may also create structural instability. The estimated relationships between GDP growth, financial conditions, and inflation may differ before and after major crises. Future research may incorporate structural break tests, regime-switching mechanisms, or time-varying parameter expectile models. Fourth, while the separate estimation of expectiles can theoretically lead to curve crossing, we have successfully resolved this issue by implementing the post-estimation rearrangement procedure of Chernozhukov et al. (2010). This ensures that the estimated lower-tail, central, and upper-tail functions maintain logical monotonicity and perfect internal consistency throughout the sample period (reducing the crossing rate to exactly 0.000). Fifth, the empirical model uses a fixed MIDAS lag length. While the selected lag length is economically interpretable, the optimal lag horizon may vary across inflation regimes. Future research may consider data-driven lag selection, penalized MIDAS structures, or Bayesian model averaging to improve lag flexibility.

To ensure that our empirical findings and policy interpretations regarding Indonesia's Inflation at Risk are highly robust and not driven by sample-specific anomalies, the empirical analysis incorporates a multi-layered robustness validation protocol. Our empirical evaluations are not conducted in isolation. Every empirical stage—including out-of-sample forecasting (Tables 9 and Table 10) and risk band diagnostics (Table 15)—compares R-MIDAS-ER against four competing econometric benchmarks (R-MIDAS-QR, R-MIDAS-OLS, AR-ER, and AGG-ER) estimated on the exact same dataset. The empirical sample is divided into an in-sample training period (2001–2019) and an out-of-sample testing period (January 2020 to June 2024). This testing period encompasses unprecedented structural breaks, including the COVID-19 pandemic, post-pandemic supply chain blockages, global energy price shocks, and aggressive global monetary tightening. Successfully navigating this highly volatile period serves as a rigorous structural robustness test for our model.

We apply the Diebold-Mariano (DM) test to the out-of-sample residuals across all models. The DM test results (detailed in Sect. 5.3) formally confirm that R-MIDAS-ER's predictive gains are statistically significant and robust, particularly in the upper tail ($\tau = 0.90$). To ensure that the estimated macroeconomic relationship in Table 14 is robust to autocorrelation and heteroskedasticity, we run a Moving Block Bootstrap (MBB) with $B = 1000$ replications. The resulting bootstrap standard errors confirm the structural stability of the estimated coefficient paths.

Overall, the empirical implementation shows that R-MIDAS-ER provides a useful framework for modeling Indonesian Inflation at Risk. Even when some benchmark models are competitive in central forecasting accuracy, the proposed model offers a more interpretable and distribution-sensitive representation of inflation risk. Its main empirical contribution lies in its ability to connect quarterly real-sector dynamics and monthly financial conditions to the evolution of lower-tail, central, and upper-tail inflation outcomes.

7 Conclusion

This study developed a Reverse Mixed Data Sampling based on Expectile Regression framework for modeling Inflation at Risk and examining the role of economic growth in shaping inflation risk dynamics. The proposed R-MIDAS-ER model was designed to address two important limitations in conventional inflation modeling. First, standard regression-based approaches are not naturally suited to accommodate mixed-frequency macroeconomic data, particularly when monthly inflation must be modeled using quarterly real-sector indicators. Second, mean-based models are unable to describe the heterogeneous behavior of inflation across lower-tail, central, and upper-tail regions of the conditional distribution. By combining the Reverse MIDAS structure with expectile regression, this study provides a flexible framework that can incorporate quarterly GDP growth into monthly inflation risk modeling while preserving the distributional nature of Inflation at Risk.

The numerical experiments demonstrate that the proposed model performs well under various residual structures, including Gaussian, heavy-tailed, skewed, contaminated, and heteroskedastic errors. These scenarios were designed to represent realistic inflation-risk environments in which macroeconomic data may exhibit non-normality, extreme observations, asymmetry, and time-varying volatility. The simulation results show that R-MIDAS-ER can recover the underlying MIDAS lag structure and produce competitive out-of-sample expectile forecasting performance. In particular, the model shows strong performance in upper-tail inflation risk regions, indicating that the integration of reverse mixed-frequency modeling and asymmetric expectile estimation is useful for identifying elevated inflation pressures. These findings confirm that the proposed framework is not only relevant for point forecasting but also valuable for distributional risk assessment.

The empirical implementation using Indonesian macro-financial data further supports the relevance of the proposed framework. The dataset consists of monthly inflation as the response variable, quarterly year-on-year GDP growth as the low-frequency real-sector predictor, and monthly financial indicators represented by the Financial Stress Index and a constructed Financial Condition Index. The descriptive analysis shows that inflation, GDP growth, FSI, and FCI are characterized by skewness, excess kurtosis, and non-normal behavior, which justifies the use of a distribution-sensitive modeling approach. In the empirical forecasting comparison, R-MIDAS-ER provides particularly useful performance in the upper-tail region, where Inflation at Risk analysis is most relevant. The model also identifies several important high-risk inflation episodes in Indonesia, including August 2013, July 2008, January 2015, and November 2022, while indicating that inflation risk became more moderate and declining toward the end of the sample period.

The coefficient path analysis provides additional economic insight. GDP growth exhibits a stronger positive association with upper-tail inflation risk than with lower-tail inflation conditions, suggesting that real-sector expansion may increase the vulnerability of the economy to high-inflation outcomes even when its effect on average inflation is limited. Meanwhile, the Financial Condition Index shows an asymmetric pattern, with negative coefficients at lower expectiles and positive coefficients at upper expectiles. This indicates that financial conditions may suppress inflation under low-inflation regimes but amplify inflation risk under high-inflation regimes through financial instability, exchange rate volatility, risk perception, and cost-push channels. The

MIDAS weighting profile also suggests that GDP growth affects inflation risk through short- and medium-term transmission channels.

Overall, the findings indicate that R-MIDAS-ER provides a useful and interpretable framework for Inflation at Risk modeling in an emerging-market economy. Even when benchmark models remain competitive in central forecasting accuracy, the proposed model offers additional value by explicitly linking quarterly real-sector dynamics and monthly financial conditions to the evolution of lower-tail, central, and upper-tail inflation outcomes. This makes the framework especially relevant for policymakers who are concerned not only with expected inflation but also with the likelihood of extreme inflationary outcomes.

Several limitations should be acknowledged. The empirical model uses quarterly GDP growth as the main low-frequency real-sector predictor, while other macroeconomic variables such as output gap, government expenditure, import prices, energy prices, food production, and external demand may also contribute to inflation risk. In addition, the constructed FCI depends on the selected financial indicators and the GARCH(1,1)-based aggregation procedure. Future research may consider alternative FCI construction methods, multiple low-frequency predictors, structural break mechanisms, time-varying parameter expectile models, monotonicity constraints to prevent expectile crossing, and data-driven MIDAS lag selection. These extensions would further improve the flexibility, robustness, and policy relevance of the R-MIDAS-ER framework for macroeconomic risk monitoring.

Acknowledgements This research is funded by the Indonesian Endowment Fund for Education (LPDP) on behalf of the Indonesian Ministry of Higher Education, Science and Technology and managed under the EQUITY Program (Contract No. 4299/B3/DT.03.08/2025 & No. 3029/PKS/ITS/2025).

Author contributions M.S.A., W.H.S., D.D.P., and A.A.K. contributed to conceptualization. W.H.S. and D.D.P. developed the methodology. W.H.S. developed the software and curated the data. M.S.A., D.D.P., and A.A.K. conducted validation. W.H.S. and D.D.P. wrote the original draft. M.S.A., D.D.P., and A.A.K. reviewed and edited the manuscript. M.S.A. and A.A.K. supervised the study. M.S.A. acquired funding. All authors reviewed and approved the final manuscript.

Data availability This study uses both simulated and empirical data. Simulated data were generated as part of numerical experiments to evaluate the finite-sample performance, robustness, and predictive reliability of the proposed model. The empirical analysis uses publicly available Indonesian macroeconomic data obtained from official public sources. The datasets are available upon request.

Declarations

Competing interest The authors declare no conflicts of interest.

Open Access This article is licensed under a Creative Commons Attribution-NonCommercial-NoDerivatives 4.0 International License, which permits any non-commercial use, sharing, distribution and reproduction in any medium or format, as long as you give appropriate credit to the original author(s) and the source, provide a link to the Creative Commons licence, and indicate if you modified the licensed material. You do not have permission under this licence to share adapted material derived from this article or parts of it. The images or other third party material in this article are included in the article's Creative Commons licence, unless indicated otherwise in a credit line to the material. If material is not included in the article's Creative Commons licence and your intended use is not permitted by statutory regulation or exceeds the permitted use, you will need to obtain permission directly from the copyright holder. To view a copy of this licence, visit http://creativecommons.org/licenses/by-nc-nd/4.0/.

References

AboAlkhair AM, Hamedani GG, Ali Ahmed N, Ibrahim M, Zayed MA, Yousof HM (2025) A new G family: properties, characterizations, different estimation methods and PORT-VaR analysis for UK insurance claims and US house prices data sets. Mathematics (Basel) 13(19):3097

Adams PA, Adrian T, Boyarchenko N, Giannone D (2021) Forecasting macroeconomic risks. Int J Forecast 37(3):1173–1191

Adrian T, Boyarchenko N, Giannone D (2019) Vulnerable growth. Am Econ Rev 109(4):1263–1289

Almetwally EM, Metwally DS, Elbatal I (2025) A new statistical model for inflation risk evaluation using actuarial techniques. Ann Data Sci. https://doi.org/10.1007/s40745-025-00644-6

Arnold B, Borio C, Ellis L, Moshirian F (2012) Systemic risk, macroprudential policy frameworks, monitoring financial systems and the evolution of capital adequacy. J Bank Financ 36(12):3125–3132

Banerjee R, Contreras J, Mehrotra A, Zampolli F (2024) Inflation at risk in advanced and emerging market economies. J Int Money Financ 142:103025

Carriero A, Galvao AB, Kapetanios G (2019) A comprehensive evaluation of macroeconomic forecasting methods. Int J Forecast 35(4):1226–1239

Chernozhukov V, Fernández-Val I, Galichon A (2010) Quantile and probability curves without crossing. Econometrica 78(3):1093–1125

Corradi V, Llorens-Terrazas J (2026) Monitoring joint tail risks: An application to growth and inflation. Journal of Econometrics 255:106237

Diebold FX, Mariano RS (1995) Com paring predictive accu racy. Journal of Business and Economic Statistics 13(3):253–263

Famubode O, Ali H (2024) The impact of the exchange rate, interest rate, and inflation on stock price. International Journal of Educational Research and Studies 6(2):70–75

Ferrara L, Mogliani M, Sahuc JG (2022) High-frequency monitoring of growth at risk. Int J Forecast 38(2):582–595

Frascaroli BF, Nobrega WCL (2019) Inflation targeting and inflation risk in Latin America. Emerg Mark Financ Trade 55(11):2389–2408

Ghysels E, Sinko A, Valkanov R (2007) MIDAS regressions: further results and new directions. Econom Rev 26(1):53–90

Ghysels E, Kvedaras V, Zemlys-Balevičius V (2020) Mixed data sampling (MIDAS) regression models. Handbook of statistics, vol Vol. 42. Elsevier, pp 117–153

Ghysels É, Santa-Clara P, Valkanov R (2004) The MIDAS touch: mixed data sampling regression models. Érudit documents and data repository (Érudit Consortium, University of Montreal). https://depot.erudit.org/id/000875dd

Ghysels E, Iania L, Striaukas J (2018) Quantile-based inflation risk models (NBB Working Paper No. 349). National Bank of Belgium

Girdzijauskas S, Streimikiene D, Griesiene I, Mikalauskiene A, Kyriakopoulos GL (2022) New approach to inflation phenomena to ensure sustainable economic growth. Sustainability 14(1):518

Khan MA, Ali H, Shabbir H, Noor F, Majid MD (2024) Impact of macroeconomic indicators on stock market predictions: a cross country analysis. J Comput Biomed Inform 8(01). https://doi.org/10.56979/801/2024

Krasniqi A, Gara A (2025) Global inflationary pressures and monetary policy response: can central banks tame the 21st century inflation? Int J Empir Econ 04(04). https://doi.org/10.1142/s2810943025500106

Li Y, Lau W-Y, Ng K-H (2025) From crisis to crisis: the moderating role of inflation and interest rate on the impact of liquidity on stock returns in selected advanced economies. Borsa Istanb Rev:100723. https://doi.org/10.1016/j.bir.2025.09.003

Lopez-Salido D, Loria F (2024) Inflation at risk. J Monet Econ 145:103570

Luo J, Fu S, Cepni O, Gupta R (2025) The role of uncertainty in forecasting realized covariance of US state-level stock returns: a reverse-MIDAS approach (Working Papers No. 202501). University of Pretoria, Department of Economics

Manzan S, Zerom D (2013) Are macroeconomic variables useful for forecasting the distribution of US inflation? Int J Forecast 29(3):469–478

Monin PJ (2019) The OFR financial stress index. Risks 7(1):25

Monteforte L, Moretti G (2013) Real-time forecasts of inflation: the role of financial variables. J Forecast 32(1):51–61

Mundra S, Bicchal M (2021) Evaluating financial stress indicators: evidence from Indian data. J Financ Econ Policy 13(1):116–135

Omer T, Månsson K, Sjölander P, Kibria BG (2024) Improved Breitung and Roling estimator for mixed-frequency models with application to forecasting inflation rates. Stat Pap 65(5):3303–3325

Saputra WH, Prastyo DD, Fithriasari K (2024a) Scenarios to handle shifts data pattern using neural network for forecasting Indonesian GDP based on financial growth at risk. In: 2024 11th International Conference on Electrical Engineering, Computer Science and Informatics (EECSI). IEEE, pp 811–816. https://doi.org/10.1109/eecsi63442.2024.10776319

Saputra WH, Prastyo DD, Kuswanto H (2024b) Machine learning modeling on mixed-frequency data for financial growth at risk. Procedia Comput Sci 234:397–403

Saputra WH, Prastyo DD, Fithriasari K (2025) An expectile-based neural network approach for mixed-frequency economic forecasting. Decis Anal J. https://doi.org/10.1016/j.dajour.2025.100666

Sarkar DR, Rao KR, Chatterjee N (2025) Crash risk assessment at unsignalized intersections using vehicle trajectory data. IATSS Res 49(4):459–469. https://doi.org/10.1016/j.iatssr.2025.09.001

Sobotka F, Kneib T (2012) Geoadditive expectile regression. Comput Stat Data Anal 56(4):755–767

Tsagkanos A, Siriopoulos C (2013) A long-run relationship between stock price index and exchange rate: a structural nonparametric cointegrating regression approach. J Int Financ Mark Inst Money 25:106–118

Vogel RM, Shallcross AL (1996) The moving blocks bootstrap versus parametric time series models. Water Resour Res 32(6):1875–1882

Xu Q, Zhuo X, Jiang C, Sun F, Huang X (2021) Reverse restricted MIDAS model with application to US interest rate forecasts. Commun Stat Simul Comput 50(2):462–482

Zakhidov G (2024) Economic indicators: tools for analyzing market trends and predicting future performance. Int Multidiscip J Univ Sci Prospect 2(3):23–29

Publisher's Note Springer Nature remains neutral with regard to jurisdictional claims in published maps and institutional affiliations.